AD-A068 777 ROYAL AIRCRAFT ESTABLISHMENT FARNBOROUGH (ENGLAND) F/G 17/7
THE MIRANDA STAR SENSOR EXPERIMENT.(U)
SEP 78 G W BROWN, P HASKELL, B HOLLAWAY

UNCLASSIFIED RAE-TR-78112 DRIC-BR-67363 NL

OF
AD
A068777

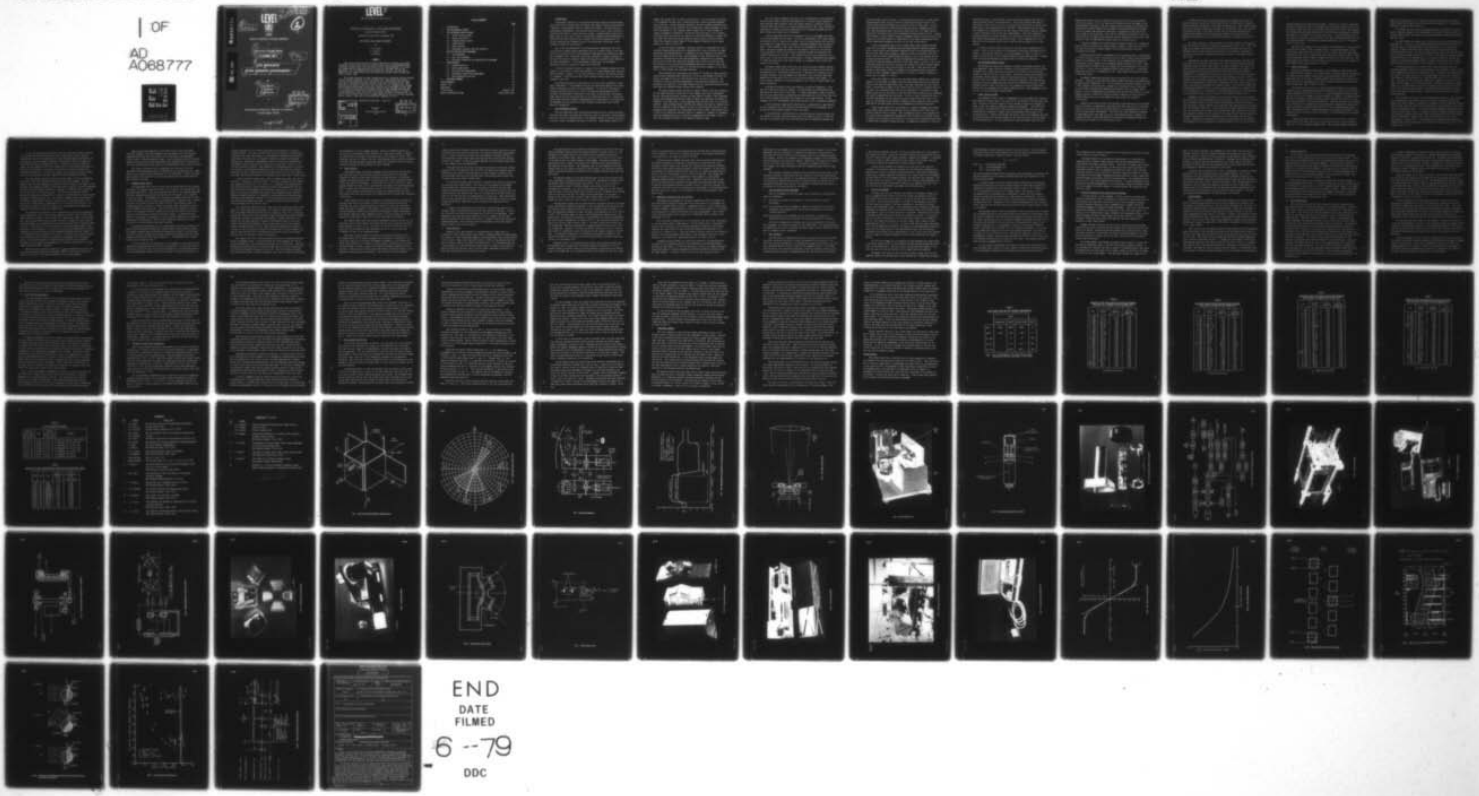

END
DATE
FILMED
6 -79
DDC

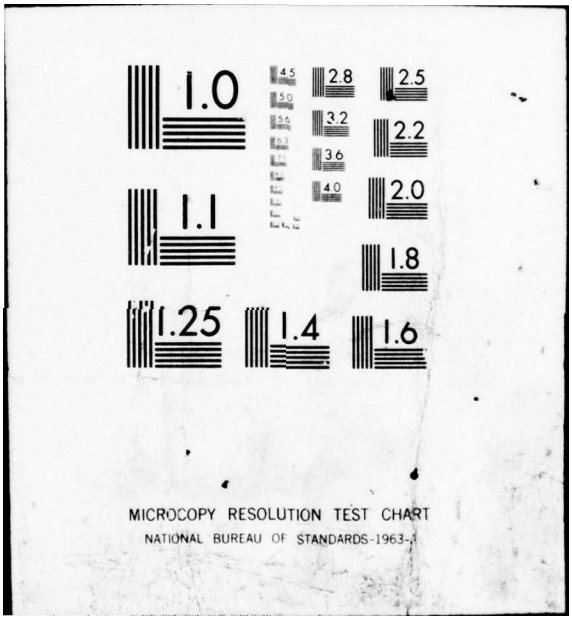
1.0
1.1
1.25
1.4
1.6
1.8
2.0
2.2
2.5
2.8
3.2
3.6
4.0
4.5
5.0
5.6
MICROCOPY RESOLUTION TEST CHART
NATIONAL BUREAU OF STANDARDS-1963-A

UNLIMITED

LEVEL II

(1)

(18) DRIC

ROYAL AIRCRAFT ESTABLISHMENT

*

(9) Technical Report 78112

(11) September 1978

(12) 73p.

(6) # THE MIRANDA STAR SENSOR EXPERIMENT

by

(10) G.W. Brown
P. Haskell
B. Hollaway

*

Procurement Executive, Ministry of Defence
Farnborough, Hants

310450

1B

LEVEL II

UDC 629.19.055.131 : 629.19.014.6

ROYAL AIRCRAFT ESTABLISHMENT

Technical Report 78112

Received for printing 7 September 1978

THE MIRANDA STAR SENSOR EXPERIMENT

by

G. W. Brown

P. Haskell

B. Hollaway

SUMMARY

This is an account of the star sensor experiment in Miranda, the British technology satellite launched by an American Scout rocket from Vandenberg AFB, California in March 1974. The star sensor used in this experiment is a single axis sensor and was designed and built at the RAE. The main aims of the experiment were to investigate the performance of the sensor in orbit and to demonstrate its compatibility with the spacecraft attitude control system when used to track a star.

The authors describe the basic design features of the sensor and the methods used to test and integrate it with the satellite. They outline the various attitude control modes that were available in orbit and describe the way these were used to acquire and lock the control system onto the selected star. The aperture of the sensor's objective lens was only 2.5 cm in diameter and although some scattered earth albedo interference occurred, many crossings of stars down to +4.5 detector magnitude were recorded during the star mapping exercises and six successful star locks were achieved on either Canopus or Sirius at roughly 1 month intervals, during the 8 month operational lifetime of the satellite. On each of these occasions the control system remained in lock for its full scheduled period of about 2 days and only unlocked when commanded to do so.

Departmental Reference: Space 558

LIST OF CONTENTS

1 INTRODUCTION

On Saturday 9 March 1974, the British Technology satellite, Miranda designated 1974-13A was launched from the Western Test Range, California and placed in a nominally sun-synchronous orbit by a NASA Scout vehicle. On board were five technological experiments, a sun pointing three axis attitude control system, an infrared earth sensor, a single axis star sensor, a digital albedo sensor and a small array of solar cells. These contained many component parts manufactured in Britain and the main objective was to assess the in-orbit performance of the various techniques and components used in each experiment during the 6 month scheduled lifetime of the satellite.

Due to the late withdrawal of two meteorological experiments, the three earth and star attitude sensor experiments were not accepted as part of the payload of this satellite until the preliminary design phase was already well underway in December 1970. Financial restrictions prevented a complete redesign of the satellite and strict spatial, weight and financial conditions were imposed on the three experiments. It was nevertheless thought that very worthwhile experiments could be carried out under these conditions.

In order to maintain accurate ($\sim$1 minute of arc) alignment between the three sensors, it was decided to mount them together in a single package which could be easily removed or replaced. It was also decided to restrict the optical testing to a minimum. As will be seen later, this involved certain risks, but these were accepted at the time.

This Report describes the objectives of the star sensor experiment, designated 'Experiment C', the equipment used and the operational modes of the control system of particular interest in this experiment. It goes on to describe the various operations carried out in orbit, including the measurement of pitch attitude, the photometric calibration of the sensor using internal and external light sources and the procedures used in star acquisition and lock. Finally the authors make their own personal recommendations for improvements in the design of the equipment and particularly for more extensive albedo glare tests during satellite integration.

2 THE EXPERIMENTAL CONCEPT

With the spacecraft pitch axis pointing towards the sun, an ideal attitude reference point about the pitch axis would be a star at the north or south ecliptic pole since it would be perpendicular to the apparent motion of the sun around the celestial sphere, throughout the whole of the year. Unfortunately there is no

bright star really close to either of these poles. The star Canopus (α Carinae) is 14.2 degrees from the south ecliptic pole and is also the second brightest star in the sky. It was therefore selected as the most suitable reference star. Its angle relative to the earth/sun line (elongation), varies throughout the year from 75.8 degrees to 104.2 degrees, hence a sensor with a field coverage of roughly 30 degrees is necessary. Polaris the north pole star, is 24.4 degrees from the ecliptic pole and is only about one tenth the brightness of Canopus and any bright star near the ecliptic equator, such as Sirius, would only remain within the elongation angle range of 75-105 degrees (covered by the 30 degree field) for 1 month in every six.

In the star sensor experiment, the basic aim was to investigate the use of an optical image splitting prism in combination with a new low resolution image dissecting type photomultiplier, to determine the star brightness and position within the sensor field of view. The advantages of this system are that it uses electronic scanning and the only moving mechanical component is the stepping mirror with its very low operational stepping rate of about one step per week. The accuracy of the star position measurements made with a sensor of this type depends mostly on the focal quality of the optics and the alignment of the prism and to a lesser degree upon the image dissector.

Some existing fully operational star sensors[1,2] already use image dissector tubes as their photoelectronic detector but so far as the authors are aware, all project the image of the star field directly onto the face of the tube. The accuracy of the star position measurements is then much more dependent on the resolution and stability of the image dissector and its associated scanning system. Such tubes are therefore larger and much more expensive.

The image splitting sensor divides its optical field in half and integrates all the light received in each half in turn, whether from star or background. The two resulting electronic currents are then added to produce a star brightness signal, and subtracted one from the other to derive star position; the former is sensitive to the mean level of the background light and the latter to its spatial gradient. When tracking Canopus therefore the optical field must be limited to an area not exceeding 15 square degrees in order to avoid excessive bias due to the background and integrated star light within the field of view. The optical field of view of the sensor was therefore fixed at 4 degrees by 3 degrees in elongation and pitch respectively and an 11 position stepping mirror was added in order to cover the 30 degree variation in the Canopus elongation angle.

The star sensor components that were to be investigated in this experiment, were an optical baffle system of RAE manufacture, a rotatable mirror mounted on jewel bearings made by Marconi Space and Defence Systems, a refractive optical system by Rank Taylor Hobson, a scanned photomultiplier by EMI, thick film hybrid electronics by Plessey, silicon photodectectors by Integrated Photomatrix and a high voltage power supply unit by McMichael.

A second important objective of experiment C was to investigate the effect of scattered sunlight on the sensor. The sun is approximately 10^{10} times brighter than Canopus and if a large area of sunlit earth is present beneath the satellite, an extensive two stage baffle is required to guarantee immunity from interfering glare. Since a baffle of this type could not be accommodated in the available space, the sensor package was mounted on the inside of one of the end sections of the spacecraft, with the star sensor projecting through the spacecraft wall furthest from the sun, see Fig 1. This allowed the wall of the spacecraft to be used as part of the star sensor baffle system. A single stage baffle was designed to reduce the glare due to the earth's albedo, to acceptable levels within the sensor field of view.

The single stage baffle fitted into the restricted space available between the satellite wall and the heat shield of the rocket nose cone, and the back wall was painted with a low reflective black paint to improve the attenuation of the scattered sunlight. This arrangement was expected to give very good shielding against direct sunlight but not to be very effective against earth albedo. It was of interest therefore to determine whether a star could be tracked under such adverse conditions.

Although the satellite orbit was planned to follow the terminator, it was obvious it would not follow it exactly. It would however be orbiting above the dark earth for about half of each orbit. It seemed reasonable to expect therefore that the star sensor would be unaffected by earth albedo for half of each orbit and with a well blackened wall might well operate for even longer periods. As the equipment was of an experimental nature this was felt to be a reasonable compromise.

A third important experimental objective was to demonstrate a simple method of star acquisition and lock using the IR earth sensor[3] for pre-alignment and to provide an eclipse warning signal for the star sensor.

As the satellite's attitude was to be controlled by an inertial system, the star sensor's attitude correction signals were only required, first to align the attitude of the system about the pitch axis and then to occasionally measure and

correct any drift about this axis. As the satellite was to fly in a near polar, sun-synchronous orbit, any star used as a pitch axis reference close to the orbital plane would be eclipsed by the earth for part of every orbit. As the star approached eclipse it would sink through the earth's atmosphere and for a short time preceding eclipse, and shortly after star rise, its light would be appreciably refracted by the earth's atmosphere (several minutes of arc). During these periods it would therefore generate alignment signals that were in error and during star fall would produce a slight drift in the control system which would then be maintained throughout the whole of the star eclipse period.

It was also possible that the star sensor might, when scanning the dark earth, see city lights resembling stars and again generate erroneous signals. Both of these effects were obviously undesirable and it was decided therefore to use one of the earth sensor signals to operate a switch to disconnect the star sensor from the control system during the whole of, and a little beyond the end of each star eclipse period. This was accomplished by mounting one of the IR detectors facing the opposite direction to the star sensor, as shown in Fig 2, the philosophy being that if this IR detector was viewing the earth, the star sensor must be pointing well away from the earth at the time. Since the earth would subtend a total angle of about 127 degrees at the planned orbital altitude of 750 km, the star alignment signals would be in control for about 36 minutes in every orbit of roughly 101 minutes.

Since there might be times in the year when glare prevented the tracking of Canopus, it was planned to attempt lock onto other bright stars such as Vega and Sirius if and when the opportunity arose. Also when searching for one of these stars, it would have to appear in the sensor field of view at a suitable point in the orbit, if a successful star lock was to be achieved. To start with it must appear during the one third part of the orbit when the IR sensor was not inhibiting the control signals from the star sensor. In fact it had to acquire the star in the first few minutes of this period in order to leave sufficient time in star lock for the Miranda control system to stabilise before going into star eclipse. Some form of attitude prediction and pre-alignment was therefore essential.

Plans already existed for the writing of a computer programme which among other things, would predict the position of the satellite in its orbit over a period of several days in advance. This information could be used together with the latest horizon crossing data generated by the IR sensor or the albedo sensor to predict the attitude of the satellite at a future selected ground station pass. It would then be possible during this pass, to command the satellite to rotate at

a given pitch rate to arrive during a later selected ground pass, with the star sensor pointing close to the selected star. The control system would then be instructed to carry out a star scan at a previously selected rate to achieve star acquisition at the optimised point in the orbit. Having locked onto the star, the alignment error registered by the star sensor could then be used as a measure of pitch attitude for use by the other experimenters. This star acquisition procedure required a suitable computer to be available on-line to carry out the many computations between one pass and the next. Such a computer was in fact available in the Miranda central control room[4] and use was made of it for this purpose.

A further relatively minor objective of the star sensor experiment was to provide a check on the accuracy of the photometric calibration procedures in use at RAE. It was planned therefore to take measurements on Vega, as this is a bright hot A0 star with a well documented absolute energy spectrum, and to compare these in-flight measurements with those taken on the RAE star simulator.

3 THE SPACEBORNE SENSOR PACKAGE

The Miranda star sensor was designed to produce two analogue outputs, the 'star magnitude' signal which was a measure of the brightness of the star and the 'alignment error' which indicated the position of the star in the pitch axis, relative to the optical axis of the sensor. Two further outputs were required by the Miranda attitude control system to facilitate star lock; these were 'star presence' and 'star trigger' and both of these were digital. Star presence was derived from the star magnitude signal and gave an indication when this voltage exceeded a preset level; the other one, star trigger, was a short timing pulse derived from the alignment error signal, generated close to and immediately prior to null, *ie* the zero voltage crossing point.

3.1 Sensor optical system

The schematic of Fig 3 shows in diagrammatic form the geometrical relationship between the sensor optics, the rear wall of the satellite and the rocket nose cone. The mirror could be rotated in steps, through an angle of 15 degrees in order to give the required 30 degrees coverage in elongation. Light reflected by the mirror, was collected by the objective lens and focused onto the plane containing the 4 degree by 3 degree focal plane aperture and the edge of the refracting prism. A Fabry lens system[5] was used to collect the emergent rays from the prism and form two stationary images of the objective lens on the face-plate of the photomultiplier. In this application it was anticipated that only one

bright star would be seen at a time and as this star moved across the optical field of the sensor, all of its light would illuminate one of the images on the photomultiplier face-plate, then as its image crossed the edge of the prism, its light would be shared between the two images on the photomultiplier face-plate. The rate at which this switchover takes place is dependent on the size of the star's image on the prism edge. This rate can therefore be adjusted to suit the control system, by slightly defocusing the optical system and in this case it was adjusted to give an approximately linear range of 12 minutes of arc.

A typical alignment error characteristic produced by Vega as it crossed the optical field of the sensor in orbital flight, is given in Fig 4 and it will be seen that the focus has changed slightly as the linear excursion was then 15 minutes of arc wide.

Calculations and previous experimental trials had shown that a 25 mm diameter f/4 optical objective used in conjunction with an 11mm f/1 Fabry lens would produce images of the required size on the face-plate of the photomultiplier and would also generate output signals with an adequate signal-to-noise ratio (SNR). When tracking Canopus, the SNR of the error signal was in fact specified to be better than 100 to 1, and on the star magnitude signal better than 150 to 1, when both signals were limited to a bandwidth of 1 Hz. These figures were easily achieved in the ground tests.

A standard commercially produced lens was selected for use as the sensor's objective. This was a Cooke Deep Field Panchro 35mm film camera lens manufactured by Rank Precision Industries Ltd. It had an effective objective diameter of 40 mm, a focal length of 100 mm and was a compound lens having good colour correction over the visible spectrum with adequate focus quality over a 25 degree field. Removal of the iris diaphragm by the manufacturers and the substitution of a fixed diameter aperture, reduced the effective entrance aperture to 25 mm, gave the required focal ratio of f/4 and enabled the lens to meet the vibration specification.

Because of the serious effect that off-axis light would have on the performance of the sensor if appreciable scattering took place from any of its internal surfaces, the lens was sent to the SIRA Institute for the measurement of its so called 'veiling glare' performance[6]. The first lens tested showed the presence of appreciable glare from light sources at field angles between 4 degrees and 20 degrees off-axis, caused principally by reflections from exposed threads and from the internal edge of the fixed aperture plate.

A modified version was therefore produced by the manufacturers with its aperture chamfered to produce a sharp edge and with the plate and the relevant threads carefully blackened by a good light absorbing paint. When tested by SIRA, this version showed a significant reduction in its internal glare. The off-axis attenuation was then of the order of about 10^6 and this was considered to be adequate when combined with the attenuation achieved by the baffle and the expected attenuation due to the wall of the satellite in shadow from the sun's rays.

The prism, situated in close proximity to the focal plane of the objective lens, had a base 11 mm long × 5 mm wide, and had angles of $30^\circ \times 30^\circ \times 120^\circ$. The ridge of the prism, which defined the null point of the sensor and hence the reference point in space about the pitch axis of the satellite, was ground to less than 5 μm and had a straightness tolerance over the 11 mm length of better than 10 μm.

Knowledge of the exact position of the star sensor optical axis about the pitch axis of the satellite, was essential in order to obtain precise pointing information from the star sensor output. The line, defined by the ridge of the prism, had to be accurately positioned and stably maintained, with respect to the mounting feet of the sensor and the prism and Fabry lens were therefore assembled in a cylindrical boss which was a precision fit in an accurately bored reference hole in the bulkhead of the star sensor casting, see Fig 5. Before assembly into the casting, adjusting screws allowed the prism carrier to be moved until the prism edge was aligned with a diameter of the boss. Once centred, the carrier was locked in position and located by dowels. The accuracy to which the prism was positioned was within ±0.01 mm, which corresponded to an angular error of ±20 seconds of arc. Limitations in this adjustment were due to the coarseness of the adjusting screws, which are shown in the assembly diagram in Fig 5.

Alignment of the prism parallel to the reference plane of the fixing feet, was carried out using the alignment jig shown in Fig 6. This jig was in two parts, the first being a base casting on which the measuring microscope was mounted, and the second, a sensor casting with a precision steel edge ground to be parallel with the reference fixing feet. With the reference sensor casting mounted on the jig, the microscope was focussed on the ground steel edge, adjusted so that movement along its lateral axis was parallel to the edge and then locked in position, thereby referencing the lateral movement of the microscope to the feet of the casting. Having set the microscope to traverse a line parallel to the plane of the reference feet, the reference casting was replaced on the jig, by the sensor

casting complete with prism and lens assembly. Rotation of the boss, containing the prism, brought the ridge into alignment with the lateral traverse axis of the microscope, after which the boss was locked and located by a dowel. The accuracy in setting up the microscope and prism was 0.005 mm, which represented a misalignment angle of ±10 seconds of arc in the pitch axis. An overall maximum error of ±0.015 mm in the setting up of the prism in the centre casting was achieved in all the qualified sensors, representing a maximum misalignment angle of ±30 seconds of arc in every case.

The Fabry lens produced two star images on the photocathode of the dissector tube that were roughly 2.5 mm in diameter with 3.0 mm spacing between centres. A small Beta light (radio active source) 3 mm in diameter and 10 mm long, which was mounted at one end of a small light pipe, was used to produce a third continuously illuminated circular image of roughly the same size as the other two. This third image was displaced to one side and in line with one of the star images, so positioning them at three corners of a square.

3.2 Sensor electronics

The image dissecting photomultiplier, type D119NMA, was developed by EMI in cooperation with the RAE. It is roughly 30 mm in overall diameter and consists of a small electron imaging section about 50 mm long mounted onto an electron multiplier about 75 mm long. A diagram showing the construction of this tube is shown in Fig 7 and a photograph of it with its mumetal housing, scan coils and high voltage power supply is shown in Fig 8.

This version of the tube has a CsSbO photocathode giving an S11 spectrum response with an average quantum conversion efficiency of about 15 per cent over a range extending from 320 nm to 540 nm. A slightly demagnified electron image replica of the optical images on the photocathode, is formed on the aperture plate and only the electrons passing through the small aperture in the centre of this plate are amplified in the electron multiplier. This has the effect of selecting only a small area of the image on the photocathode for transmission and the dark emission current is therefore much lower than in the standard photomultiplier tube. The application of a deflecting magnetic field allows the position of the selected area to be shifted so that the whole of the photocathode can be scanned if necessary.

A hole 2 mm (0.08 inch) square in the aperture plate defines a sensitive area 2.9 mm (0.114 inch) square at the photocathode because of the demagnification of 0.7 in the electron imaging system. The electrons passing through the

aperture are multiplied in an 11 stage box and grid dynode structure which has highly stable CsSb surfaces at each stage, giving a high gain at a relatively low operating voltage of about 1000 volts.

The D119NMA tube was specially ruggedised by EMI to withstand the environmental conditions imposed by the launch phase of the mission and was potted in silicone rubber inside the mumetal housing which provided screening from external magnetic fields.

The high voltage power supply was a proprietary unit type 9782 produced by McMichael Ltd. It was of a light weight annular potted construction made to fit round the base of the photomultiplier and consisted of a dc to dc converter producing a highly stabilised output voltage controlled by an external low voltage reference source. The output voltage could be varied from 500-1500 volts with a reference voltage change of 3.5-7.5 volts. The latter was adjusted during calibration to give the required gain in the electron multiplier and when set, the high voltage output remained stable to within ±0.25 per cent when the input supply varied from 20.5-28 volts and the temperature varied from -20 to +70°C.

A detailed description of the basic star sensor electronics has been published elsewhere[7] and only a brief description will therefore be given in this Report commencing with the block diagram of Fig 9. The split star image produced two beams in the image section of the photomultiplier and these were sampled in time sequence by the application of a switched 128Hz magnetic field on one axis only. The beam from the calibration image was not sampled at the same time as these, but was sampled in an alternative mode of operation available on command. Simple scan circuits generated the binary waveform current that was fed to one coil of the deflection coil assembly. The spacecraft clock provided a 1024Hz clock pulse which was divided down to produce the 128Hz scan and the required gating waveforms.

The resultant pulse train at the photomultiplier anode, was first amplified and then gated into two separate channels, one where the pulses from the two images were added together to produce star recognition and star magnitude signals, and the other, where the pulses were subtracted one from the other to produce the error or misalignment signal. Since the operations programme required the star sensor to measure and lock on to a number of stars of different magnitude during its lifetime, automatic gain control (AGC) was incorporated in the error signal channel to maintain a constant slope over the linear portion of the error characteristic shown in Fig 4. An Analogue Devices divider AD530 provided the required AGC, to limit variations on the output to less than 2 per cent for input changes of up to 5 to 1.

In the star lock mode of operation, the star sensor was directly connected to the spacecraft attitude control unit (ACU), whose pitch control loop was switched into and out of eclipse mode by a star presence signal, generated by the star sensor. The star presence signal was gated into the ACU by a signal from the IR horizon sensor, Experiment B (IR4). In addition to the star presence signal, the ACU required a star lock trigger pulse to initiate the final phase of the star lock manoeuvre. The arrival of this pulse in the ACU, switched the difference between the star sensor error signal and the pitch gyro error voltage into the pitch updating loop, and released the pitch integrator from hold.

The star presence signal was derived from the output of the star magnitude channel by a four level threshold detector, set by ground command. Any star brighter than the preset magnitude, produced a direct voltage at the output of the detector that triggered a Schmitt circuit and held it on until the star disappeared. The output from the Schmitt trigger was combined in a NAND gate with the IR4 output to produce the star presence signal. Provision to override the eclipse warning IR4 signal was incorporated, to prevent a possible failure in the IR sensor permanently prohibiting star lock. The star-lock trigger pulse was generated by two Schmitt triggers which detected a voltage level on the linear part of the sensor error characteristic, approximately ± 1 volt from the null position. Outputs from the Schmitt circuits were gated into a monostable which produced the required 30 ms duration star-lock trigger pulse.

The photometric sensitivity of the photomultiplier plus the star magnitude channel amplifiers could be monitored by sampling the light output from the Beta-light calibration source. This was achieved by applying a current to the lateral axis scan coils and deflecting the normal scan line to sample two other areas of the photocathode, one illuminated by the Beta-light and the other a dark unilluminated area. Subtraction of the dark response from the Beta-light response, gave a measure of the system gain. To carry out the calibration measurement, a ground command was sent which switched the star magnitude amplifier from an 'adding' to a 'subtracting' mode and applied the dc bias to the lateral axis deflection coils. This calibration could not give any indication of degradation of the optical system. The overall response was therefore monitored with a star simulator throughout the pre-flight test programme and by reference stars such as α Lyrae (Vega) during the flight programme.

Hybrid circuit technology, established in Space Department and used in the very successful Hybrid Electronic Experiment (HEE)[8] in the Prospero satellite, prompted the choice of this form of assembly for the X4 experiments.

Apart from the head amplifier and the AGC circuit of the star sensor electronic package, the active components and the greater part of the passive components were built into five hybrid circuit substrates, each measuring 56 mm × 32 mm × 4 mm and weighing 12 grams. These were mounted with the external components onto printed circuit boards which were assembled into a box construction on a sub-frame that fitted around the photomultiplier tube as shown in Fig 10.

The control electronics for the stepping mirror were built into two additional hybrid substrates which are described in the following section. Manufacture of six types of hybrid substrates for the integration, flight and flight spare sensors, was carried out by the Plessey Company and the seventh type was made in-house at the RAE.

3.3 Stepping mirror system

The requirement for a mirror to step the star sensor field of view through an angle of ±15 degreees about the normal to the satellite sun pointing axis, has been mentioned earlier. This facility allowed any star of the required magnitude, having an elongation angle between 70 degrees and 107 degrees, to be acquired by the star sensor. The maximum rate of change of elongation angle for any star to which the sensor could be locked, was approximately 1 degree per day. Individual steps of the mirror rotated the sensor field of view through an angle of 3 degrees giving an overlap of 1 degree on adjacent steps and complete coverage of the required field in ten steps. With this overlap the command to step the mirror to an adjacent position, during star lock, was not critical and could be sent any time during one of several consecutive passes. An additional step, added at a late stage in manufacture, to give a twelfth position, was achieved by adjusting the limiting stop. This was used during the launch phase to give protection to the photocathode from direct sunlight.

The design and manufacture of the stepping mirror system was carried out by Marconi Space and Defence Systems Ltd, Frimley (MSDS) under a contract whereby the stepper mechanism and test boxes were manufactured by MSDS. The associated electronic circuits designed and developed by MSDS were manufactured into hybrid packages by the RAE and the Plessey Company Ltd. A photograph of the stepping mirror system is shown in Fig 11.

To avoid vignetting and degradation in the alignment of the sensor optical system, the reflecting plane of the mirror was required to be positioned close to the axis of rotation of the mirror and be perpendicular to the mounting surface of the stepping mirror system. The mirror was made of fused silica ground to a

flatness tolerance of $\lambda/8$, surface aluminised and protected by a coating of silicon monoxide. The plate, on which the mirror was mounted, was fitted with collinear pivot steel pins running in 2.5mm diameter instrument jewel bearings which were selected to give the requisite freedom of movement with minimum bearing slop. Mechanical indeterminancy, about the pitch axis perpendicular to the mirror's axis of rotation, was required to be less than 10 seconds of arc and this was easily achieved. When assembled, the perpendicularity of the axis of rotation to the mechanism mounting face, had to be such that the reflected beam from the mirror, when the mirror was rotated from one end of its travel to the other, did not move relative to the mounting face by more than 1 minute of arc.

A space qualified stepper motor, with a 90 degree step angle, was fitted with 60 to 1 gearing to drive the mirror. The latter consisted of two stages of spur gearing with ratios of 6 to 1 and 10 to 1 to minimise its dimensions and low friction materials, Delrin and Nylatron GS were used respectively for the gear wheels and the intermediate shaft bearings to obviate the use of lubricants which, in the space environment can migrate and contaminate optical surfaces. Despite the high coefficient of expansion of these materials, carefully chosen tolerances gave sufficient clearances to allow operation within specification, over the required temperature range. A diagram showing the mirror mounting, encoder and gear train is shown in Fig 12.

The encoder was required to give a read out of the angular position of the mirror in a Gray code using a different 4 bit number for each mirror position, with each number differing from the next by a change in only 1 bit. An optical encoder was chosen and by using very small light emitting diodes (LED) and photo-transistors low mass, size and power was achieved. A major reduction in the overall size was made possible by using the intermediate shaft to drive the encoder disc which was designed to have a single track for all four channels within a maximum diameter of 25 mm. When the mirror movement was extended to 12 steps, it was not possible to modify the encoder disc to give a unique 4 bit word for that position and it was accepted that the read out for the twelfth position would be identical to that for position 11.

The stepper motor has two phase windings which must be energised simultaneously for maximum torque. To conserve power they were energised for 100 ms, at each required step, the system being quiescent at all other times. Each motor winding was connected across a transistor bridge that was in turn controlled by a J-K bistable through isolating gates (Fig 13). The two bistables, together with some steering logic, formed a reversible ring counter in which the direction

was determined by the two command channels. These two command channels also controlled a pulse generator which produced the clock pulse required to operate the ring counter and trigger a monostable with a pulse length of 100 ms. This monostable was used to 'enable' the four isolating gates and so allow the bistables to switch, through subsequent amplifying stages, the appropriate arms of the two transistor bridges and thus energise the motor windings.

3.4 Baffle system

The planned flight operations programme included quite long periods with the satellite's pitch control system locked onto the earth and it was hoped therefore to observe as many stars as possible during this part of the flight schedule and thus provide accurate attitude fixes and a fairly continuous record of the star sensor's performance. In this mode, the yaw (-z) axis was to point roughly towards the centre of the earth and the star sensor was therefore mounted with its optical axis 20 degrees above the roll (-x) axis, as shown in Figs 1 and 2. As the horizon was expected to be about 26.5 degrees below the x-axis, the optical axis would then be about 46.5 degrees above the horizon when operating in this mode.

When tracking a star in star lock mode, the sensor would be pointing away from the earth and at an altitude of 750 km, the IR4 infrared sensor would disconnect the control signals whenever the sensor's optical axis approached closer than about 53 degrees to the horizon. The earth lock mode thus imposed the more difficult problem and the baffles were designed to begin attenuating any incident light more than 2 degrees off axis in the pitch plane and to have reached an attenuation of about 10^4 at an off axis angle of 40 degrees.

The largest baffle unit that could be accommodated between the wall of the satellite and the launch vehicle heat shield was one 5.5 cm long with a rectangular aperture, 6.6 cm by 2.9 cm. This gave the required attenuation about the pitch axis and also gave the same attenuation of 10^4 on a source more than 45 degrees off axis in the elongation plane.

There was an area of about 320 sq cm of satellite wall bounded by the ±40 degree pitch and ±45 degree elongation cut off angles of the baffles. At a fairly late stage in the satellite development programme, it was decided that silver foil would have to be added to various areas on the back wall and on the yaw jet housing, in order to achieve the required operating temperature of the satellite. Great care was taken to keep these highly reflective surfaces as far outside the sensitive areas as possible. Even so with the lowest possible

surface reflectivity of about 1 per cent achieved by the best black paint on this sensitive area, the overall attenuation of the optical system and the blackened wall, to light incident on this area was only expected to be about 10^8 and it was obvious that earth albedo light reflected from this surface would interfere with the star signal. It was not however expected to be at a high enough level to cause damage to the photomultiplier.

When orbiting the dark earth, the optical system with its off-axis attenuations of 10^6 in the objective lens and 10^4 in the baffle unit together with the shielding of the satellite structure gave more than adequate protection from direct sunlight and also from a distant sunlit horizon when this was more than 40 degrees below the sensor's optical axis.

The only other bright sources liable to interfere with the star signal were the moon and sunlit space debris. The latter was not expected to be present except perhaps for a few brief periods occurring in the first few days after launch and could therefore be ignored. It was also planned to select a star for attitude control that would be well clear of the moon and on the dark side of the orbit for the few days that the system would be in star lock. There would therefore be quite long periods in each orbit when the system would be able to operate without interference, sufficient in fact to achieve the objectives of the experiment.

To simplify the manufacture of the baffles, the shroud was made as four separate plates, each plate having six knife edge baffles 10 mm deep. In Fig 14 the four plates are shown with the jigs used to carry out the machining. After machining, the plates were black anodised to act as a primer, and the inner surfaces sprayed with 3M's Black Velvet paint to produce a matt black surface for maximum absorption. The four plates were then assembled to form the complete baffle system as can be seen in Fig 15.

3.5 Glare detector

Exposure of the photocathode of a photomultiplier to high levels of illumination, when a high voltage supply (EHT) is applied between the photocathode and anode, will cause irreparable damage to the photocathode. This can be prevented if the source of light can be detected, before it falls on the photocathode, and used to operate a shutter to obscure the light from it. An alternative solution to this problem is to use the detected light signal to operate a power switch to remove the EHT from the tube, and in the star sensor experiment the latter of these two solutions was used to protect the tube.

The glare detector was an additional sensor mounted on the base of the star sensor experiment directly above the entrance aperture, as shown in Fig 15. The 90 degree by 45 degree field of view and the level of sensitivity were both designed so that bright light sources were detected before they were near enough to the optical axis, or bright enough to cause damage. Any source generating a photocurrent above a preset value operated a transistor switch that removed the EHT from the photomultiplier. The subsequent loss of star recognition and error signals from the star sensor, initiated a logic process in the satellite attitude control loop which returned the satellite to the inertial reference mode about the pitch axis.

The sensing elements in the glare detector were two low noise silicon photocells, developed by Integrated Photomatrix Ltd (IPL), measuring 9 mm square, each one having a dark resistance greater than 100 MΩ. These cells were mounted in the focal planes of twin f/1 optical systems, each having a field of view 45 degrees by 45 degrees. The centre of the detector's field of view was aligned with the centre of the star sensor field of view, with the ±45 degree field centred about the pitch axis and the ±22.5 degree field centred about the yaw axis. A sketch of the optical system is shown in Fig 16 which shows the two 11mm focal length Spectrosil lenses with their respective silicon photocells.

Circumstances dictated that the glare detector electronics should be designed round a preselected operational amplifier, a set of preferred value resistors, and an interface with a transistor switching circuit, already frozen in design. To meet the operational temperature range, the gain of the amplifier had to be limited to 500×10^6 volts per ampere in order to avoid significant changes in the triggering level, resulting from variations in the amplifier off-sets with temperature. The final circuit configuration is shown in Fig 17. The operational amplifier was used in an 'off-set' mode, giving a logic '1' at point B when the detectors were not illuminated. Radiation exceeding the triggering level falling on one or both of the detectors, resulted in the output at point A falling to -8 volts or below, and a logic '0' appearing at point B, switched off the supply voltages to the EHT unit. If excessive illumination of the detectors saturated the amplifier, the resistor R6 limited the current that could be drawn from the transistor switching circuit to an acceptable level.

Simulation tests in the laboratory and further tests viewing the moon from the RAE Observatory, showed that any visible radiation exceeding 5.10^{-9} W cm^{-2}, incident within the optical field of the glare detector, would switch off the EHT. Tests on a D119NMA tube in an experimental sensor also showed that this was a safe

level as no deterioration of the photocathode was observed with incoming radiation of this intensity. This level is roughly equivalent to the energy received from a half moon and is ten times less than a full moon.

Previous work by Brookman[9] had shown that, from a satellite orbiting above the earth's terminator, the reflection coefficient on the sunlit side of the terminator would be about 1 per cent and the reflected solar radiation from this area of the earth would therefore be about 14 watts per sq metre. At this level of radiation, the earth's sunlit horizon had only to be inside the glare detector field of view by a few minutes of arc to switch off the EHT. This system also gave full protection of the photomultiplier from brightly lit space debris appearing anywhere within its field of view. Radiation reflected from the back wall of the satellite was prevented from operating the glare protection system, by masking the appropriate detector as shown in Fig 18. This was a mistake, not realised at the time, as it is now believed that some damage to the photomultiplier may have occurred as a result of this masking. This will be discussed in more detail later.

3.6 Mechanical interface with the satellite

Maintaining the alignment of the sensor through the severe environment of the launch phase required the main frame of the star sensor to be strongly reinforced but to remain light in weight. A magnesium alloy 'L' section casting with a central bulkhead, strengthened about the root of the cantilever by a 'U' section and reinforced by a closely fitted cover, met these requirements. The construction of the star sensor and the layout of its components parts is shown in the photograph in Fig 19.

Pitch attitude information was to be provided by the star sensor 'Experiment C', the IR horizon sensor, 'Experiment B', and the albedo sensor, 'Experiment D'. Accurate cross reference of the attitude measurements between the three sensors required that their fields of view, be mutually aligned and maintained to an accuracy of ±1 minute of arc. Since the required accuracy could not be achieved by mounting the three experiments individually on the spacecraft structure, it was decided to mount them onto a common mounting plate as shown in Fig 15.

Alignment accuracy between the sensors was achieved in the manufacture of the plate by fine tolerances placed on the machining of the mounting surfaces provided for each sensor. It was also achieved by the use of a webbed structural design which gave the required dimensional stability and kept the weight within the limit imposed. A reference cube fitted on the plate permitted optical

measurement of the alignment of the three experiments with respect to each other. Spacecraft axes were defined by a reference cube mounted on the gyro pack to which both the fine sun sensor and the reference cube of the experiment package were aligned. Accuracy of alignment of the experiment package to the spacecraft axes was required to be within ±0.5 degree, measured to an accuracy of ±2 minutes of arc, for each of the three axes. In practice an alignment accuracy of ±0.25 degree was readily obtained on both the integration model and the flight equipment.

The experiment package was mounted on the underside of the top floor of the spacecraft as shown in Fig 20 with the star sensor on a cantilever mounting and its longitudinal axis parallel to the spacecraft pitch axis. Mounting the package in this position enabled the star sensor to project beyond the surface of the spacecraft furthermost from the sun, and allowed the variable position mirror to be mounted in the projecting part of the sensor.

4 TEST AND QUALIFICATION PROGRAMME

The test programme for the star sensor can be divided into three distinct areas of requirement:

(i) The detailed testing of the sensor as a unit to assess its overall performance.

(ii) The qualification test programme to assess the stability of the sensor's performance and alignment under the simulated conditions of launch and in-space operation.

(iii) The integration test programme with the spacecraft to establish the compatability and correct operation of the sensor/spacecraft interfaces.

Of the four completed star sensors, only two were subjected to the whole test programme, the integration model and the flight model. The engineering model was tested only as a unit to establish the basic design and the flight spare model was not integrated into a spacecraft.

4.1 Test equipment

Two test boxes were manufactured and used to operate the star sensor under electrical conditions identical to those encountered in the spacecraft. The first test box was developed for the manufacturing stage of the sensors and could test individual hybrid circuits as well as the completed sensor[7]. The second, shown in Fig 21, was specifically designed to test the complete sensor only and was made portable for ease of handling between the test facilities at the RAE,

at HSD Limited, Stevenage, and also for the pre-launch check out, at the Western Test Range, California. Spacecraft interfaces simulated by the portable test box were the 1024Hz clock pulse, supply voltages, telemetry and commands. In addition to these an array of lamps indicated the logic status of the sensor, and test points were provided for measuring the sensor analogue outputs.

A small special purpose star simulator was also built, that could be attached to the satellite support structure for use during the integration and qualification testing of the fully equipped satellite. This device simulated a single star of Canopus magnitude and was used as a routine check of the alignment and sensitivity of the star sensor throughout the satellite test programme. The RAE star sensor test facility[10-12] where stars of accurately known magnitude can be simulated and scanned through small angles up to 2 degrees, was used in the more detailed unit performance development and calibration tests.

4.2 Unit test programme

In these tests the star simulator was adjusted to simulate a single star with no background light present and the star sensor was mounted so that the star scanned across the central region of its field of view, about the sensor's pitch axis. This enabled measurements to be made of the outputs of the error and star magnitude channels, which were recorded on a calibrated XY plotter against star misalignment angle. These measurements were repeated for different magnitudes of simulated stars, and also for different parts of the field of view by adjustment of the star sensor position in both axes. Monitoring of the sensor temperature and EHT output was carried out throughout the tests. A typical XY plot of the error characteristic at one fixed mirror position is reproduced in Fig 22. This shows the variation in the error signal over a range of sensor magnitudes (m_s) from -1.41 to +0.10. It will be seen that the error characteristics for star magnitudes covered by this range, were indistinguishable from each other over the linear portion of the characteristic about the null position. Variations in the slope of this characteristic of up to 5 per cent, were recorded over the complete 30 degrees elongation field of view covered by the stepping mirror.

The star-lock trigger was also checked by super-imposing this output pulse on the error signal record, as the simulated star was scanned through the sensor field in both directions. From this record, the position with respect to the null, the amplitude and the duration of the trigger pulse was measured.

Throughout this series of tests the direct output voltage from the star magnitude channel was recorded and a curve, showing this voltage plotted against

star brightness in sensor magnitude units is shown in Fig 23. The sensor magnitudes were based on the visual magnitude (-0.73) and spectral energy distribution of Canopus as measured for NASA by Forbes[13] using the formula

$$m_s = m_v + CI$$

where m_s = star sensor magnitude
m_v = visual magnitude, and
CI = the colour index.

The colour index was derived from the spectral energy distribution of Canopus, the spectral sensitivity of the sensor photomultiplier and the transmission of the sensor optical system.

To prevent noise on the star presence signal interrupting the connection between the sensor and the control system during star lock, some hysteresis was deliberately introduced into the threshold circuit to give ~2 to 1 difference (~0.75 m) between star seen and lost trigger levels. The ability to vary the magnitude of the simulated star continuously, allowed the four threshold detector settings and the hysteresis on each setting to be measured. The star presence lamp on the test box was used to show the points at which star presence was gained and lost. Simulation of the eclipse warning signal was also incorporated in the test box and this enabled the override eclipse warning command channel to be checked.

The procedure used to check the alignment of the star sensor was as follows; the collimated beam of the star simulator was first adjusted to be horizontal with the aid of a theodolite; the sensor was then mounted on a rotary table that could be tilted, and with the aid of an accurate clinometer to measure the angle of tilt, the sensor axis defined by the null position, was measured with respect to the reference mounting feet. An assessment of errors in the various instruments, placed a tolerance of ±0.25 minute of arc on the final measurement. In the case of the flight model sensor the null axis was measured and found to be offset by an angle of 3.5 ± 0.25 minutes of arc. This did not change as a result of the environmental testing. Using the same techniques the fields of view of the sensor were measured utilising the two rotations of the table. The resultant measurements are shown diagrammatically in Fig 24.

It was a general requirement laid down by the spacecraft design authority that the power, mass, centre of gravity, moment of inertia and electrical bonding of the experiments be measured and maintained within limits defined by them.

These properties were therefore measured for each individual star sensor and some of the results are shown in Table 1.

The same authority also specified the requirements for sinusoidal and random vibration, thermal vacuum, thermal soak and rapid depressurisation at qualification and flight acceptance levels. These were all normal space qualification tests in every respect except one and this was the rather high level of sinusoidal vibration that the equipment was required to meet. This level was increased from 30 g to 40 g peak over a frequency range of 65-100 Hz at a fairly late stage in the development programme and proved difficult to meet, within the permitted weight restriction, with the prototype design. The problem was solved by the use of a well ribbed magnesium alloy chassis. A special dispensation was granted for the maximum temperature to be used during storage and thermal cycling. Due to the danger of possible damage to the photocathode, this temperature was limited to $+50^{o}C$.

4.3 Satellite integration and qualification programme

At various points in this programme, a series of optical and electrical checks was performed in order to determine the viability of the various units in the satellite, and these were carried out step by step by automatic computer controlled checkout equipment using a programme known as SOLACE (satellite orientated language for automatic checkout equipment). These tests included some specifically designed to monitor the operation of the 'live' star sensor. In addition to the standard power supply, telemetry and telecommand checks, all the sensor analogue and digital output signal levels were tested, as a routine procedure, using both the internal Beta light and the small Canopus star simulator as input light sources.

Dynamic testing of the sun and star sensor interfaces with the attitude control systems of the two spacecraft were carried out on the satellite ACS test facility at the RAE. Because the motion simulator was a single axis one, these tests were carried out in two steps, one with the satellite mounted on its base and the second with it turned over on its side, for the pitch and yaw control system tests respectively.

The vacuum chamber surrounding the simulator was too small to contain the sun and star simulators inside it and both were therefore mounted outside. A free standing star simulator was used to produce a collimated beam of light which was aligned with the star sensor line of sight, through an optically flat window in the wall of the vacuum chamber. The spacecraft, mounted in a frame on the

table of the motion simulator, was commanded to rotate about its pitch axis, at different rates, so that the simulated starlight would pass across the sensor field of view and so check the correct operation on the ACS/star sensor interface in the different spacecraft modes of operation. Although the sun simulator was available, it was not switched on during the star locking tests as the glare situation would have been totally unrepresentative in such conditions and would have completely inhibited the operation of the system.

An initial scan at orbital rate, 217^{o}/h, was performed to verify the correct operation of the star presence and star-lock trigger signals. Once it was established that the sensor/spacecraft interface was operating correctly, the spacecraft was commanded into star acquisition mode and star lock was effected at both orbital rate and at 20^{o}/h, from both directions. When the spacecraft was in space-lock, the star signal was removed to simulate the star eclipse mode of operation and it was established that the spacecraft switched automatically into inertial hold and back again to star lock when the signal returned. The other star mapping and scanning modes of operation were also checked.

5 FLIGHT RESULTS

With the satellite orbiting in continuous sunlight and the control system held on continuous sunlock about two of its axes throughout its lifetime, the only degree of freedom available to the star sensor experiment was the ability to rotate the satellite about its pitch sunpointing axis. There were four modes of operation of the pitch control system that were of major interest to the star sensor experiment and these were 3, 5, 5A and 6. In mode 3 the satellite could be rotated continuously at one of many rates selected from a limited number of fixed ones of 0, ±8, ±12 and $\pm 217^{o}$/h used in any combination, together with a digitally variable one, within the range +30 to -30^{o}/h with a resolution of 12 binary bits, *ie* to 1 part in 4096.

Mode 5 was the star tracking one and was itself divided into three subsidiary modes, star search, star lock and star eclipse, the last being known as mode 5A. Only the fixed rates were available for star search mode and zero rate was used in the other two. Mode 6 was the star scanning one and always followed immediately after a period of operation in mode 5. A square wave rate demand of $\pm 8^{o}$/h peak amplitude was applied to the control system and was timed to give a ±1.2 degrees scan centred on the star that had been used as a reference in the previous star lock mode. This mode was used to exercise the star sensor at a sufficiently slow rate in order to obtain a detailed telemetry plot of the sensor's characteristics.

5.1 Delayed switch-on

It was possible during launch, while the third stage was still spinning, that the star sensor might point directly at the sun for several minutes. If the sun's rays were focussed directly onto the photomultiplier during this period, its photocathode would almost certainly be damaged. The satellite was therefore launched with the sensor power supplies switched off and with the stepping mirror parked in its extreme off-axis position. The sensor was not switched on and the mirror rotated into its operational position until it had been confirmed that a stable lock onto the sun had been achieved. Due to gas control problems, this event did not take place until 3 days after launch.

This delayed switch-on also reduced the possibility of corona damage to the photomultiplier EHT supply. No attempt had been made to make the outer casing of the sensor air tight so that it could be operated without trouble in a normal earth atmosphere and at the very low air pressures in space. However this method of construction introduced the possibility of damage if the supply is operated at the intermediate air pressures in the range 10^{-1} to 10^{-3} torr therefore the delayed switch-on served to obviate this risk.

5.2 Earth albedo glare

The satellite was rotated at many different rates when calibrating the gyro control system[14] and when exercising the IR and albedo sensors. On most of these occasions the star sensor was pointing at the earth for a large part of every orbit. This was also true when the satellite was in star lock and for this reason the star sensor operation was inhibited for quite long periods during these exercises. However at intervals of about 1 month or so throughout the flight programme, star mapping exercises were carried out with the star sensor pointing well away from the earth throughout each such exercise. In the absence of glare from the satellite structure, the sensor would then have remained operational over the whole of each orbit, but this proved not to be the case. It was found in fact, that the sensor operation was inhibited by earth albedo, not only when orbiting directly over the sunlit earth, but also when orbiting a little beyond the terminator. Fig 25 shows typical operational periods in a few selected star mapping orbits and the incidence of glare inhibition. The sensor was never operational within the area on the diagram marked 'glare inhibited', either in star mapping exercises, or in any of the other modes, including the star tracking ones. It was also sometimes inhibited by glare outside this area, as shown by gaps in the solid lines in Fig 25, which indicate star mapping exercises, and the situation was therefore a little worse than expected, but not excessively so.

In order to appreciate the sources of glare from the satellite structure and the earth's albedo it is necessary to consider the geometrical relationship between the satellite's orbital plane and the sun. This plane rotated about the earth's polar aixs at roughly the same rate as the apparent movement of the sun, slightly slower in fact, by about 2 degrees per month, and it did not follow the sun at all in a north-south direction. The perpendicular to its orbital plane continued to point 7.8 degrees north of the equator for the whole of the operational lifetime of the satellite.

During the period of the first star search on the 21 March 1974 (day No.80), the sun was over the equator and the terminator was then passing through the north and south poles as shown in Fig 26a. The Miranda orbital plane was tilted 7.8 degrees beyond the north pole and was lagging behind the sun by about 1 degree in the equatorial plane. The satellite was therefore travelling over the dark earth on the north going part of the orbit when passing near the north pole. Fig 25 shows that the sensor was switched on and operating correctly during this part of the orbit, at this time of the year, even though the satellite was fully illuminated by the sun at the time.

With the satellite in its sun-synchronous orbit, the solar arrays were continuously illuminated by the sun, from launch until towards the end of its operational lifetime when the satellite started going into eclipse. The solar cells were very thin and made of silicon and were therefore fairly transparent. Fig 26a therefore demonstrates that none of the sunlight transmitted through the solar array affected the sensor and that the main source of glare was the reflection of earth albedo from the back of the satellite or some projection on it.

The orbital plane came closest to the terminator on about the 10 April as it was then perpendicular to the sun in the north/south plane and lagging by about 2 degrees in the east/west direction. The intermittent operation of the sensor over the period about the 30 April shown in Fig 25, shows that the sensor was still affected by albedo glare when orbiting close to, but on the dark side of the terminator.

During the summer the North Pole was illuminated by the sun and the South Pole became dark and the sensors operational periods obviously changed in sympathy with this, see Fig 26b. By the end of September the plane of the orbit was lagging behind the sun by about 20 degrees and the intermittent performance of the sensor observed in springtime was therefore not repeated in the autumn, as the orbit was then crossing the terminator at a larger angle.

The period in each orbit when Vega, Sirius and Canopus would have been available for star lock, had glare not been present, has been indicated on Fig 25. This diagram thus shows the extent to which glare reduced the availability of these two stars for use as a star lock reference.

5.3 Pitch attitude measurement

In the star mapping exercises, the yaw axis was pointed towards the centre of the earth and the star sensor scanned a 360 degrees strip of the celestial sphere 4 degrees wide, over a circle that rotated in space about the earth's polar axis by approximately 1 degree per day. By using the stepping mirror facility, the 4 degrees strip could be moved in 3 degree steps to any one of 11 adjacent positions to give a total available strip of sky 34 degrees wide. In this mode of operation, the sensor was scanning the sky at a rate of 3.6 minutes of arc per second and any star crossing the sensor field of view produced, in 50 seconds, about six telemetered voltage samples, in recorded data from each of the two analogue signals, star magnitude and alignment error. The passage of a point source such as a star could therefore be easily recognised and isolated from other more diffuse sources of light, both by the number of recorded samples of each pulse and also by the rapid positive and negative excursions of its alignment error voltage (see Fig 4).

A computer programme[15] was used to produce an attitude model of the satellite from the albedo and IR sensor data, using the latest available orbital elements, to convert earth based coordinates into spatial ones. This model was then used to compute where the optical axis of the star sensor was pointing in coordinates of right ascension and declination and these were printed out with each telemetered measurement of star magnitude and alignment error voltage. The values of right ascension and declination associated with a null in the alignment error voltage, gave the approximate position of the star, to within a degree on the celestial sphere and it was then relatively easy to identify each star by name and number from a standard star atlas or catalogue. Several stars were often observed in one orbit and their identity was checked by correlating the timing of their null points with their known relative pitch angle spacings.

Four of these star mapping programmes were carried out between mid-April and the latter part of August and a total of 80 or more stars down to a detector magnitude of +4.5 were observed in this way. All these stars are listed in Tables 2 to 5 in order of brightness. The spectral classifications and the visual magnitudes are given from the Yale catalogue[16] and the detector magnitudes were calculated from these using the S11 photocathode colour indices published

in an earlier report[17]. All the star pairs detected as single stars, had separations of less than 40 seconds of arc.

As the linear part of the alignment error characteristic was approximately 12 minutes of arc wide and the telemetry samples occurred at intervals of 8 seconds, at earth rotation rate, the chances of any one sample occurring within the 3.3 second duration of this linear excursion was low. The accuracy of the attitude fixes in this mode of operation were therefore not accurate, the maximum error being about ±15 minutes of arc. They did however provide a very useful cross-check on the satellite attitude computations based on data from the other sensors, especially in the first few months of flight when the operation of the gas jet system[14,15,18] was a little erratic. The albedo sensor data processing technique was for instance, found to be unreliable and gave misleading attitude information[14,15] at times but the IR sensor data processor was very good.

Having identified the stars and established an accurate attitude model for the satellite, it was then relatively easy to identify these and other stars seen when the satellite was rotating much more slowly. Accurate attitude fixes to within 1 minute of arc were then available for use by the other experimenters during the slow rolling mode of operation and also of course when the system was in star lock. However, the low sampling rate of the earth sensor data and its timing made it impossible to correlate this data with that from the star sensor to a better accuracy than a few minutes of arc.

5.4 Photometric sensitivity measurement

Most of the prelaunch photometric measurements were carried out using the Beta-light as a reference source and with the sensor operating at a temperature of about 20°C, as measured by means of a telemetered thermocouple mounted close to the photocathode of the photomultiplier. Some measurements were however performed over a -10°C to +40°C range during flight qualification thermal cycling tests and these showed that the sensor star magnitude output had a photometric temperature coefficient of 0.0128 V/°C or approximately 0.25 per cent of full scale per °C. The in-flight temperature, measured by the same thermocouple, varied from 0°C to +10°C and all the photometric calibrations quoted, have therefore been normalised to +5°C.

All the photometric measurements were transmitted via the star magnitude analogue telemetry channel with an estimated overall transmission accuracy of approximately 1 per cent, *ie* to ±0.05 volt and each measurement plotted in Fig 27 is a mean of several hundreds of individual measurements taken over one or more orbits.

A Beta-light calibration check carried out only 4 days after launch showed that the launch of the satellite into space had no obvious effect on the sensitivity of the photomultiplier or the signal amplifiers. A few intermittent checks up to late June showed a slight, rather variable fall in photomultiplier sensitivity and by this time it had reached a mean value about 12 per cent down on the prelaunch value. From then on right through to satellite eclipse in November, the photomultiplier sensitivity as measured by the Beta-light, remained at roughly this same mean value but fluctuated fairly widely between limits of 7.8 and 17.5 per cent down on its prelaunch value.

Three very bright stars Vega, Canopus and Sirius were used as alternative standard photometric sources during the operational lifetime of the satellite, the choice depending on their availability within the operational field of the sensor at each particular time, that is to say they were within the range of the stepping mirror and were visible from the satellite when orbiting over the dark earth. Vega was the first one to be seen, 12 days after switch on and the sensor's photometric sensitivity already showed an apparent drop of 10 per cent compared with the ground calibration figure obtained on the star simulator before launch. Measurements on Vega over the following 12 days showed a fairly steady deterioration to a value 27 per cent below ground calibration.

Some recovery was observed when Canopus was first observed on day 109 with a measured sensitivity only 16 per cent down, but further photometric calibrations using Canopus and Sirius as reference sources over the following week, gave a wide and erratic variation ranging from 16-36 per cent down. From this point onwards the sensor's photometric sensitivity fell rather erratically till by the end of September it had reached a figure 75 per cent down from its prelaunch value.

Analysing the telemetry records more carefully, it became obvious that the star calibrations were very dependent on the immediately preceding glare situation. This was demonstrated very clearly on day 113 during measurements on Canopus. On the last two consecutive morning passes, the star magnitude output from Canopus was only 15 and 18 per cent below the prelaunch value. On the first evening pass, the telemetry records showed that the sensor had been exposed to glare and the photomultiplier EHT had been overloaded for about 14 minutes just before Canopus entered the field of view and this resulted in a measurement 34 per cent down.

It will be remembered that the light from the Beta-lamp was focussed onto a different part of the photocathode to that entering the sensor through its optical system. It seemed likely therefore that the slight fall in the Beta-light sensitivity measurements was due to a reduction in the secondary emission from the

surface of the dynodes while the much larger change in star sensitivity was mainly due to a similar deterioration in the two star image areas of the photocathode. All the emissive surfaces of the cathode and dynodes in the D119 NMA tube are caesium activated and it is well known that caesium ion migration from these surfaces, occurs under overload conditions. It is also known that partial recovery of sensitivity will take place due to a gradual remigration of the ions if the phototube is 'rested' in the dark for several days.

Tests on the spare engineering model sensor were therefore carried out in the laboratory under conditions representing those in flight and it was demonstrated that the resultant effects were very similar to those observed in flight. It was also shown that partial recovery did in fact occur if the tube was 'rested'. In order to test this hypothesis it was therefore arranged that the star sensor in the Miranda satellite be switched off for 5 days in the middle of October. A Beta-light and a Sirius calibration were both carried out immediately before switch-off and immediately after switch-on and a recovery in sensitivity of some 7-16 per cent was noted thus supporting the above hypothesis. Though not conclusive it is now confidently believed that the glare detector was not quite sensitive enough and the area of the detecting element in the glare detector viewing the part of the satellite within its field of view should not have been blacked out, Fig 18. These are both faults which could be corrected in any future design.

5.5 Star acquisition and lock

It would have been possible to acquire a star and lock onto it by starting star search at any arbitrary pitch angle, but the probability of a successful lock onto the star chosen by the experimenter, would not have been very high in such circumstances. This was partially due to the fact that the control system was designed to switch into star lock immediately the sensor saw any fairly bright star whose light, plus that of the background, exceeded the set brightness threshold. There was thus a distinct possibility that, if the system had to scan through an area of sky such as the Milky Way, it would lock onto a weaker star in this area instead.

As mentioned earlier, it was also essential that the sensor's optical axis cross the star sight line at a point in the orbit which left sufficient time for the control system to settle down before going into eclipse. Due allowance also had to be made for the fact that the system could only be switched into its star search mode, and therefore had to begin its search, when the satellite was passing over Lasham. By manoeuvring the satellite into a more favourable attitude

with the star sensor pointing fairly close to the chosen star and by using a fairly slow search rate, quite a high success rate has been achieved.

Because the satellite was sun-synchronous with its orbital plane roughly perpendicular to the sun throughout its operational lifetime, it passed over the ground transmission and reception station at Lasham in two or three consecutive orbits near dawn and dusk every day. No other ground station was used in the Miranda operations and there was therefore no opportunity to command or receive data except during these two daily groups of passes. The routine procedure used to achieve star lock was therefore as shown in the diagram of Fig 28.

Though not essential, but merely for operational convenience, it was usually arranged for star acquisition to take place between two early morning passes and the necessary operational control procedures always started 24 hours earlier. These began by setting the pitch rotation rate to zero on the last pass of this previous morning and the latest available telemetry data were examined in order to confirm that the glare situation was satisfactory and were also used to make preliminary attitude computations.

Two convenient points in time T_1 and T_2 were selected by the flight operations controller for the transmission of telecommands changing the pitch rotation rate. The time T_1 was chosen to occur during the second pass in the evening of the first day and the second time T_2 was always in the first pass of the following morning. Fairly accurate timing of these transmissions to within a minute or so of the planned time was essential if a successful acquisition was to be achieved.

During the 100 minute orbital period prior to T_1 the computer was programmed first to take the orbital parameters and calculate the place where, and the point in time T_3, when star lock would take place, assuming a search rate of $20^{\circ}/h$ would be used between times T_2 and T_3. Having fixed T_3, the required attitude at the time T_2 could then be calculated. Finally the attitude of the satellite at time T_1, predicted from the latest available IR data and orbital parameters was used to calculate the prealignment rotation rate required during the period T_1 to T_2. This rate was transmitted to the satellite and put into operation at time T_1. The computer was also programmed to calculate the optimum mirror position and if a mirror adjustment was required, this was commanded during the same pass.

The $20^{\circ}/h$ rate was put into operation when the satellite was switched into mode 5, at time T_2. The control system was then in its star search mode and

star lock occurred later in the orbit, quite close to the predicted time T_3. By the time it reached Lasham on its next pass, the control system was usually operating in inertial hold, mode 5A, due to the temporary eclipse of the star, and the system then continued to switch automatically from this mode into star lock and vice versa on each subsequent orbit, without intervention from ground control.

An early attempt at star lock during the fourth week in orbit was unsuccessful mainly because glare was, at that time, severely restricting the length of the sensor 'on' time. As a result Canopus could not be seen at all and the Vega signals were only available for some 15 minutes or so in each orbit. The pitch gyro had not been calibrated in flight and albedo horizon crossing data were being used in the attitude calculations. As a result attitude errors of several degrees were present. However trial runs across Vega suggested that star lock might be successful and an attempt was therefore made to lock onto this star on day 94 (4 April). Unfortunately star lock occurred rather late in the orbit and star control was only maintained for a few minutes before sensor shut down occurred due to eclipse. As a result the control system drifted during eclipse and although Vega was still in view on the next orbit, it was too far off axis for the system to recover.

At this point it was decided to wait a few weeks until the orbit had moved away from the terminator and the sensor switch-on periods had become longer, before attempting a second star lock. Advantage was also taken of this break to modify the computer programme, making it accept the more accurate horizon crossing data generated by the IR experiment in place of the albedo generated data and so improve the accuracy of the attitude calculations to better than 1 degree. This break also gave sufficient time for a long series of gyro drift rate and scale factor calibration exercises to be carried out.

By the middle of May the glare situation had improved considerably and it was therefore decided to attempt star lock once more. Vega was out of range of the sensor's optical field, its elongation was too large and it would not come back within range until September but Canopus was now being observed by the sensor for about 20 minutes in each orbit. A Canopus lock was therefore attempted on day 142 (22 May) and this was very successful, the system being allowed to stay in lock for a period of 4 days. Throughout this period the sensor indicated a steady bias of about 1 minute of arc misalignment from the star sight line, with minor noise angle fluctuations about this mean of about 0.1 minute of arc rms.

Star lock was repeated from this point on, at roughly 1 monthly intervals with no further problems, as listed in Table 6. These star locks were successful inspite of the apparent fall in sensor sensitivity and in the slope of the alignment error voltage at null, see Table 7. The wide variation in the latter was due to the limited range of the automatic gain control circuit which was not designed to cope with star magnitude signals of less than 1.0 volt. The figures in the tables show that satisfactory star locks were still achieved with null slopes of about 0.4 volt per minute of arc, (Canopus, day 211, E1; Canopus lock, day 212) well below its prelaunch value of 0.78 volt per minute of arc and its specified minimum of 0.58 volt per minute of arc.

At the conclusion of two successful star locks on Sirius on days 261 and 286, the system was commanded on each occasion, to go into star scan, mode 6, in order to obtain a detailed plot of the sensor's error voltage/misalignment angle characteristic. This was found to have changed very little if at all, since launch and with the stronger Sirius signal the slope at null was back to normal as shown in Table 7.

6 CONCLUDING REMARKS

The late acceptance of the attitude sensing experiments as part of the Miranda satellite payload resulted in some compromise in their design. They had to fit into an existing satellite layout with strict weight limits imposed on them; they had to withstand quite high levels of vibration, and restrictions on data rate which, limited the accuracy that could be achieved in the correlation of their various pitch attitude measurements. The size of baffle that could be used on the star sensor was strictly limited and as a result, earth albedo scattered from the surfaces of the satellite, adjacent to the star sensor, was detected by the sensor when it was orbiting over the sunlit earth. However inspite of all these difficulties, a very successful series of experiments was carried out. Star signals that were generated when the satellite was orbiting over the dark earth were used to derive accurate pitch attitude fixes for use by the other experimenters and a reliable method for the control of the pitch attitude of a sun-pointing satellite was demonstrated.

The Miranda flight trials have shown that an optical image splitting system used in conjunction with a relatively simple inexpensive image dissecting photomultiplier, is a promising technique offering considerable potential for the accurate sensing of star position. The resulting star sensor has been shown to be relatively small, 41.2 cm by 10 cm by 9 cm, light in weight, 3.6 kg, to have a low power consumption, 2 watts, and to be cheap to manufacture.

112

A glare sensor was included as part of the star sensor package and this was designed to switch off the sensitive photomultiplier whenever excessive glare was present. The satellite was launched in a polar orbit and as a result any star used for pitch attitude control was eclipsed by the earth for a considerable part of each orbit. A technique was therefore developed using the signal generated by one of the IR experiment detectors, together with that of the glare sensor, to ensure that the star sensor signals were connected to the inertial control system only during the 'safe' part of each orbit. This often restricted the time available for star acquisition to about 20 minutes in each orbit.

The Miranda control system required about 15 minutes to acquire the star and settle down into a steady state star lock, before the star signal disappeared, due to eclipse by the earth, as it might otherwise have drifted during the following 80 minute period when no star signal was available and then have lost the star when it re-emerged from eclipse. An on-line computer in ground control was therefore programmed to take the telemetered earth sensing data as it became available (from the IR experimental sensor), together with the latest available orbital parameters, and to make the necessary pitch attitude predictions that enabled ground control to rotate the satellite into a suitable position to give rapid acquisition of the star at the correct point in the orbit. Using this method, the Miranda control system was locked onto Vega, Canopus and Sirius on several different occasions and stayed on-lock for several days each time.

Many stars were also observed during the periods when the satellite was rotating at earth orbital rate. Some 83 stars were seen and identified during these star mapping operations, ranging from -1.41 to +4.54 in detector magnitude. Many star attitude fixes were therefore available during these and other operational programmes, but attempts made to compare the pointing accuracy of the star sensor with that of the IR sensor Experiment B, were limited by the telemetry sampling rate and timing system to an accuracy of a few minutes of arc.

Some deterioration in the sensitivity of the star sensor took place during the 8 month operational lifetime of the satellite. By the fourth month its sensitivity had fallen to about 25 per cent of its prelauanch value but remained thereafter, for the last 4 months of its operational life at about this same level. However design tolerances were such that the sensor continued to produce useful star data and provide satisfactory star lock right up to the end when the satellite itself went into solar eclipse and ground control was lost.

The cause of the fall in sensitivity is not known for certain. There are many possible explanations such as contamination or radiation damage of the

optics, electronic amplifier gain changes and overload or thermal damage to the photomultiplier, but a careful analysis of the telemetry records together with ground tests on a spare sensor have shown that the most likely cause was overload damage due to inadequate protection of the photomultiplier by the glare sensor.

It is possible that such a fault went unobserved during ground integration tests due to the omission of any full-scale glare trials on the satellite. Such tests would have been very difficult to carry out due to the relatively high level of the simulated sunlight scattered from the walls of any existing vacuum chamber; nor could such a test be carried out outside of a chamber as the light scattered by the air would then be too great. The extensive modifications to a vacuum chamber to carry out these tests would have been expensive and would have taken a long time to install and test. They were therefore ruled out for both these reasons. In the opinion of the authors the results more than justified the risks that were taken. Such tests should however be given very serious consideration in any future proposal to use a star sensor in a spacecraft especially if there is any doubt about the effectiveness of the baffle system and a high reliability and long life of the star sensor are required.

Another solution would be to use a much larger two-stage optical baffle unit and to ensure that no part of the satellite is within the cut-off angle of such a unit. There is then a more difficult problem of siting the star sensor on the spacecraft structure, but if this can be solved, the performance of the star sensor will be completely independent of the reflections from any part of the satellite. If, as in the case of Miranda, the available space in the nose cone is very restricted, it should be possible to develop a collapsible baffle unit, that can then be erected in space.

Acknowledgments

The authors would like to thank EMI Ltd for their permission to reproduce the diagram of the photomultiplier tube type D119 shown in Fig 7. They would also like to take this opportunity to acknowledge the efforts put into the manufacture of the sensors by Mr W. Hollingworth of Space Department, Design Office, and by the Workshop staff of the RAE under the supervision of Mr R. Goswell, in particular Mr E. Board and Mr A.E. Lusty for their assistance in the assembly of the sensors. Finally they would like to thank Mr J. Cram resident EQD Inspector for his advice and supervision during the programme.

Table 1

STAR SENSOR POWER AND MASS PROPERTY MEASUREMENTS

	Model			
	Integration	Flight	Flight spare	Units
Mass	3682	3682	3683	g
Power	2.065	2.024	1.842	W
CG (xx)	-	51	50	mm
CG (yy)	-	40	38.5	mm
CG (zz)	-	209.5	209.2	mm

Note. The CG measurements were made from the same stipulated reference surfaces on each sensor

Table 2

IDENTIFIED STARS FROM FIRST STAR MAPPING PROGRAMME.
DAYS 109-119, 19 APRIL 1974 TO 29 APRIL 1974

Star	Spectral class	Visual magnitude	S11 detector magnitude
α CMa	A1 V	-1.47	-1.41
α Car	F0 Ib	-0.73	-0.36
ε CMa	B2 II	1.50	1.10
γ^2 Vel	WC7 + O7	1.82	1.20
δ CMa	F8 Ia	1.84	2.56
α Pav	B3 IV	1.93	1.57
β Gru	M3 II	2.24	4.24
ζ Pup	O5 f	2.25	1.62
η CMa	B5 Ia	2.40	2.10
π Pup	K5 III	2.70	3.93
α Tuc	K3 III	2.85	4.03
α Hyi	F0 V	2.86	3.23
O^2 CMa	B3 Ia	3.04	2.68
γ Hyi	M0 II	3.24	4.54
α Dor	A0 si	3.26	3.26
α Ret	G6 II	3.34	4.29
β Dor	F8 Ia	3.40	4.12
β Pav	A5 IV	3.42	3.65
χ Car	B2 IV	3.46	3.06
ε Gru	A2 V	3.48	3.60
δ Pav	G8 V	3.55	4.31
β Pic	A3 V	3.84	4.03
κ CMa	B2 Ve	3.96	3.56
γ Tuc	F0 III	3.98	4.35
β Oct	d A9	4.14	4.50
*β^1 Tuc	B8 V	4.36	4.22
*β^2 Tuc	A2 V	4.53	4.65
δ Tuc	A2 V	4.46	4.32

* Detected as one star.

Table 3

IDENTIFIED STARS FROM SECOND STAR MAPPING PROGRMME
DAYS 149-160, 29 MAY 1974 TO 9 JUNE 1974

Star	Spectral class	Visual magnitude	S11 detector magnitude
α Car	F0 Ib	-0.73	-0.36
α Eri	B5 IV	0.47	0.17
α Leo	B7 V	1.36	1.17
β Car	A1 IV	1.67	1.73
γ^2 Vel	WC7 + O7	1.82	1.20
ε Car	KOII + B	1.85	2.85
δ Vel	A0 V	1.95	1.95
α Hya	K4 III	1.99	3.28
ζ Pup	O5 f	2.25	1.62
λ Vel	K5 Ib	2.30	3.53
α Phe	K0 III	2.39	3.39
μ Vel	G5 III	2.68	3.56
β Hyi	G2 IV	2.79	3.51
α Hyi	F0 V	2.86	3.23
*ν Car	A9 II	3.15	3.51
*ν Car	F0	6.03	6.40
α Pic	A5 V	3.26	3.49
α Dor	A0 si	3.26	3.26
β Phe	G8 III	3.30	4.24
χ Car	B2 IV	3.46	3.06
ϕ Vel	B5 II	3.53	3.23
ϕ Eri	B8 V	3.55	3.41
o Vel	B3 III	3.61	3.25
α Pyx	B2 III	3.68	3.28
s Car	F0 II	3.82	4.19
p Vel	F2 + A3	3.83	4.25
a Vel	A0 II	3.90	3.90
e Vel	A9 II	4.13	4.49
b Pup	B3 V	4.49	4.13

* Detected as one star.

Table 4

IDENTIFIED STARS FROM THIRD STAR MAPPING PROGRAMME
DAYS 195-201, 14 JULY 1974 TO 21 JULY 1974

Star	Spectral class	Visual magnitude	S11 detector magnitude
α Car	F0 Ib	-0.73	-0.36
α Vir	B1 V	0.96	0.50
β Cru	B0.5 IV	1.24	0.73
*α^1 Cru	B1 IV	1.58	1.12
*α^2 Cru	B3n	2.09	1.73
γ Cru	M3 II	1.62	3.62
β Car	A1 IV	1.67	1.73
ε Car	KOII + B	1.85	2.87
δ Vel	A0 V	1.95	1.95
θ Cen	KOIII-IV	2.05	3.05
γ Cen	A0 III	2.16	2.16
ι Cav	F0 I	2.24	2.61
ε Cen	B1 V	2.30	1.84
κ Vel	B2 IV	2.49	2.09
ζ Cen	B2 IV	2.54	2.14
γ Crv	B8 III	2.60	2.46
μ Vel	G5 III	2.68	3.56
ι Cen	A2 V	2.76	2.88
δ Cru	B2 IV	2.82	2.42
δ Crv	B9.5 V	2.95	2.89
β Mus	B2.5 V	3.04	2.64
α Dor	A0 si	3.26	3.26
ω Car	B7 IV	3.31	3.12
**θ^1 Eri	A3 V	3.42	3.61
**θ^2 Eri	A2	4.42	4.54
χ Car	B2 IV	3.46	3.06
ϕ Vel	B5 II	3.53	3.23
ϕ Eri	B8 V	3.55	3.41
p Car	B5 Ve	3.58	3.28
o Vel	B3 III	3.61	3.25
†μ^1 Cru	B3 IV	4.02	3.66
†μ^2 Cru	B5 Ve	5.18	4.88

* Detected as one star
** " " " "
† " " " "

Table 5

IDENTIFIED STARS FROM FOURTH STAR MAPPING PROGRAMME
DAYS 234-238, 22 AUGUST 1974 TO 26 AUGUST 1974

Star	Spectral class	Visual magnitude	S11 detector magnitude
α Car	F0 Ib	-0.73	-0.36
β Ori	B8 Ia	0.08	-0.06
*α^1 Cen	G2 V	0.33	1.04
*α^2 Cen	dK1	1.70	2.54
β Cen	B1 II	0.59	0.13
β_1 Cru	B 0.5 IV	1.24	0.73
**α^1 Cru	B1 IV	1.58	1.12
**α^2 Cru	B3 n	2.09	1.73
γ Cru	M3 II	1.62	3.62
β Car	A1 IV	1.67	1.73
ε Car	KOII + B	1.85	2.87
ε Cen	B1 V	2.30	1.84
α Lup	B2 II	2.30	1.90
η Cen	B1.5 V	2.35	1.89
ζ Cen	B2 IV	2.54	2.14
α Col	B8 Ve	2.63	2.49
α Mus	B3 IV	2.71	2.35
θ Car	09.5 V	2.76	2.17
δ Cru	B2 IV	2.82	2.42
β TrA	F2 IV	2.84	3.26
γ TrA	A1 V	2.88	2.94
α Dor	A0 si	3.26	3.26
γ Ara	B1 III	3.33	2.87
†41 Eri	B8.5	3.55	3.41
†43 Eri	M1 III	3.96	5.44
p Car	B5 Ve	3.58	3.28
ϕ Cen	B2 IV	3.82	3.42
J Cen	B5 V	4.52	4.22

* Detected as one star
** " " " "
† " " " "

Table 6

STAR ACQUISITION AND LOCKS

Start of star lock		Star	End of star lock		Remarks
Day	Pass		Day	Pass	
94	E2	Vega	94	E3	Lock lost during eclipse period
142	E3	Canopus	146	E1	Commanded out of star lock
183	E2	Canopus	184	M3	Commanded out of star lock
212	E2	Canopus	213	M3	Commanded out of star lock
213	E2	Canopus	214	M2	Commanded out of star lock
259	M2	Sirius	261	E1	Commanded into mode 6
285	M3	Sirius	286	E1	Commanded into mode 6

Table 7

VARIATION OF ERROR CHARACTERISTIC SLOPE WITH STAR MAGNITUDE OUTPUT

Day	Pass	Star	Star magnitude output volts	Error characteristic slope Volts/minute
88	E3	Vega	1.12	0.627
89	E2	Vega	1.15	0.677
140	E2	Canopus	1.18	0.562
211	E1	Canopus	0.71	0.403
230	M1	Canopus	0.86	0.513
232	E2	Canopus	0.63	0.349
232	E3	Canopus	0.63	0.381
240	E2	Canopus	0.79	0.479
249	E2	Canopus	0.83	0.483
261	E2	Sirius	1.61	0.675
261	E2	Sirius	1.65	0.717
261	E3	Sirius	1.61	0.777
261	E3	Sirius	1.69	0.753
303	M1	Vega	0.35	0.197

REFERENCES

No.	Author	Title, etc
1	A.J. Smets P. Van Dijk W.J. Christus	The optical sensors of the Netherlands astronomical satellite ANS. (1974) Philips Technical Review, Vol 34 (1974)
2	R.A. Deters D.F. Eisenhut R.F. Gates	The fine guidance sensor, an electronic scanning star tracker. ITT Federal Laboratories, San Fernando, California, US
3	M.B. Barnes S. Craig A. Haskell	The Miranda (X4) infrared experiment: design performance and earth radiance measurements. RAE Technical Report 77161 (1977)
4	E.A.R. Anstey M.J. Hammond	Real time operational control of Miranda. RAE Technical Report 76016 (1976)
5	John Africano Robert Quigley	What is a Fabry lens? Sky and Telescope, Vol 54, No.1, pp 60-62, July 1977
6	S. Martin	Glare characteristics of two Cooke photographic lenses for use in a star sensor. SIRA Institute, report No.G380 (1972)
7	H.W. Brown	The electronics of the star sensor in the British satellite, Miranda. RAE Technical Memorandum Space 216 (1974)
8	P. Clarkson	Hybrid electronic experiment on board Prospero. RAE Technical Report 72221 (1973)
9	A.K. Brookman	The Prospero satellite attitude sensing system. RAE Technical Report 73117 (1973)
10	B. Hollaway	Star sensor test facility at the RAE. RAE Technical Report 71091 (1971)
11	A.G. Gleave	The alignment and photometric calibration of a star and skylight simulator. RAE Technical Report 70037 (1970)
12	A.G. Gleave	Star simulator calibration based on the spectrum of Vega. RAE Technical Report 72138 (1972)

REFERENCES (concluded)

No.	Author	
13	R.J. Mitchell F.F. Forbes H.L. Johnson	Spectral energy distributions for bright stars in watts cm^{-2} nm^{-1}. Private communication.
14	W.G. Hughes	Operational experience of the Miranda (X4) satellite attitude control system. RAE Technical Report 75116 (1975)
15	J.I. Thomas	Performance of the 100 element albedo sensor experiment on the satellite Miranda (X4). RAE Technical Report 77102 (1977)
16	D. Hofleit	Catalogue of bright stars (third revised edition 1964). Yale University Observatory (1964)
17	P. Haskell	Star tables for satellite attitude control. RAE Technical Report 68048 (1968)
18	-	Miranda X4 - in orbit performance assessment report. Hawker Siddeley Dynamics in conjunction with RAE (1974)

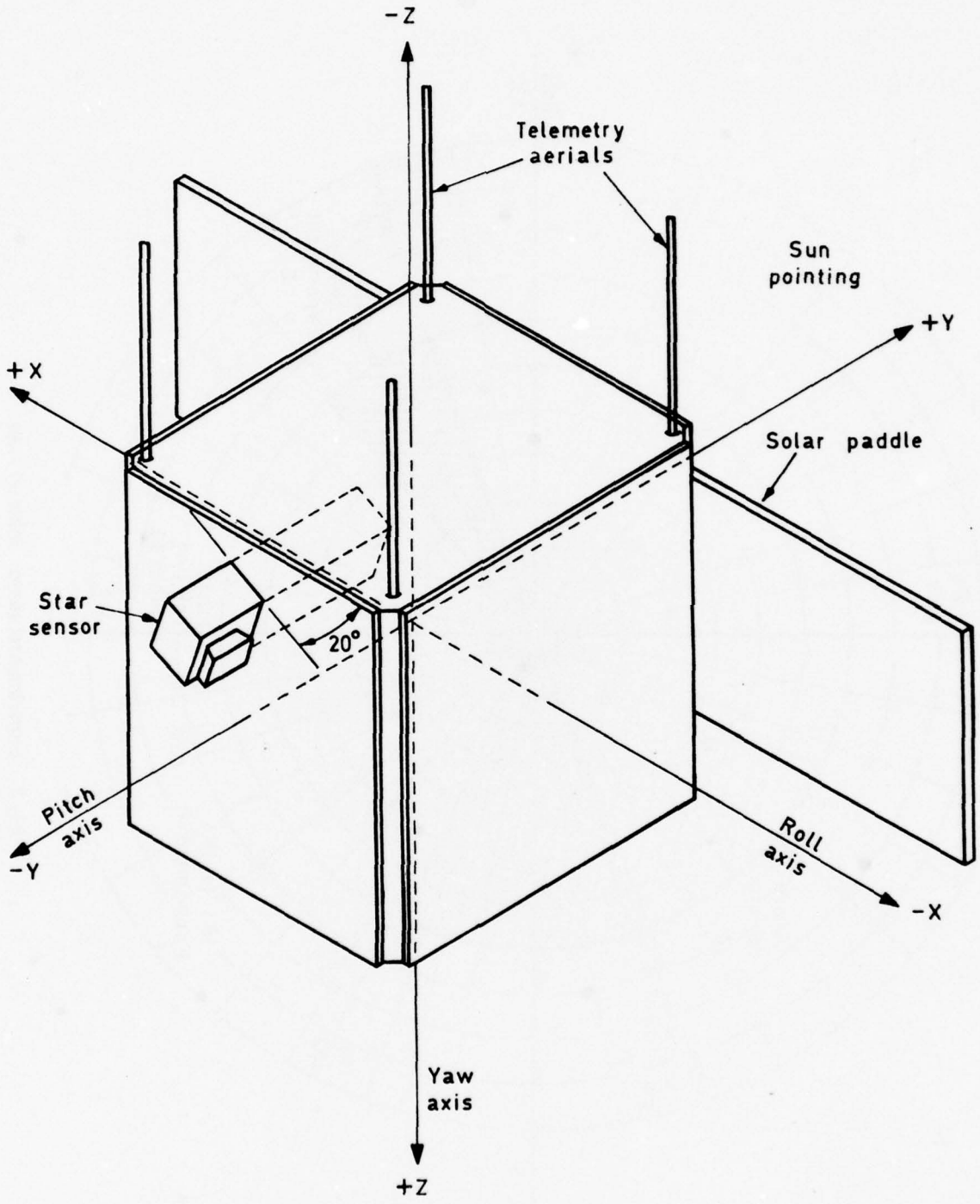

Fig 1 Star sensor position relative to spacecraft axes

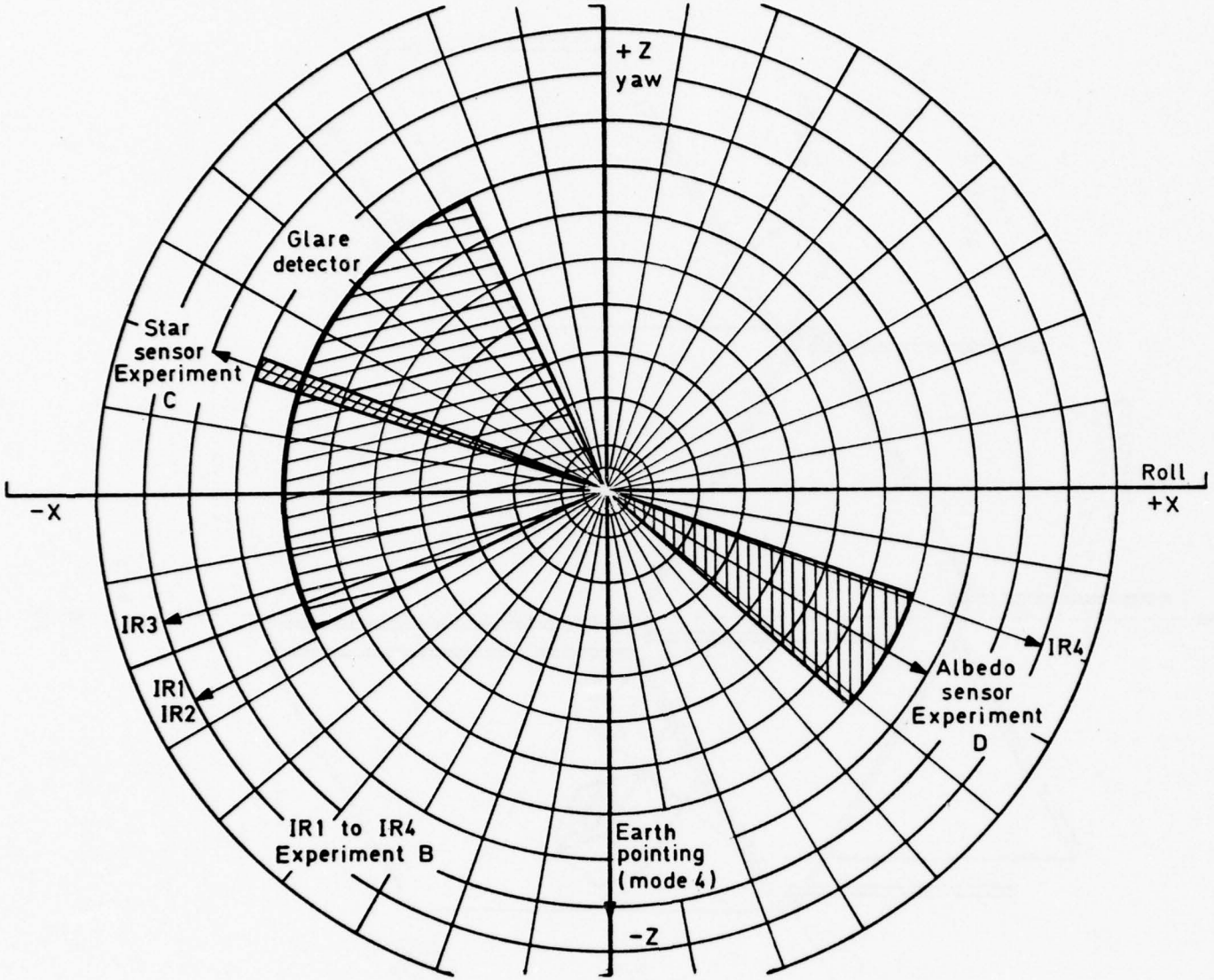

Fig 2 Experimental sensor fields of view

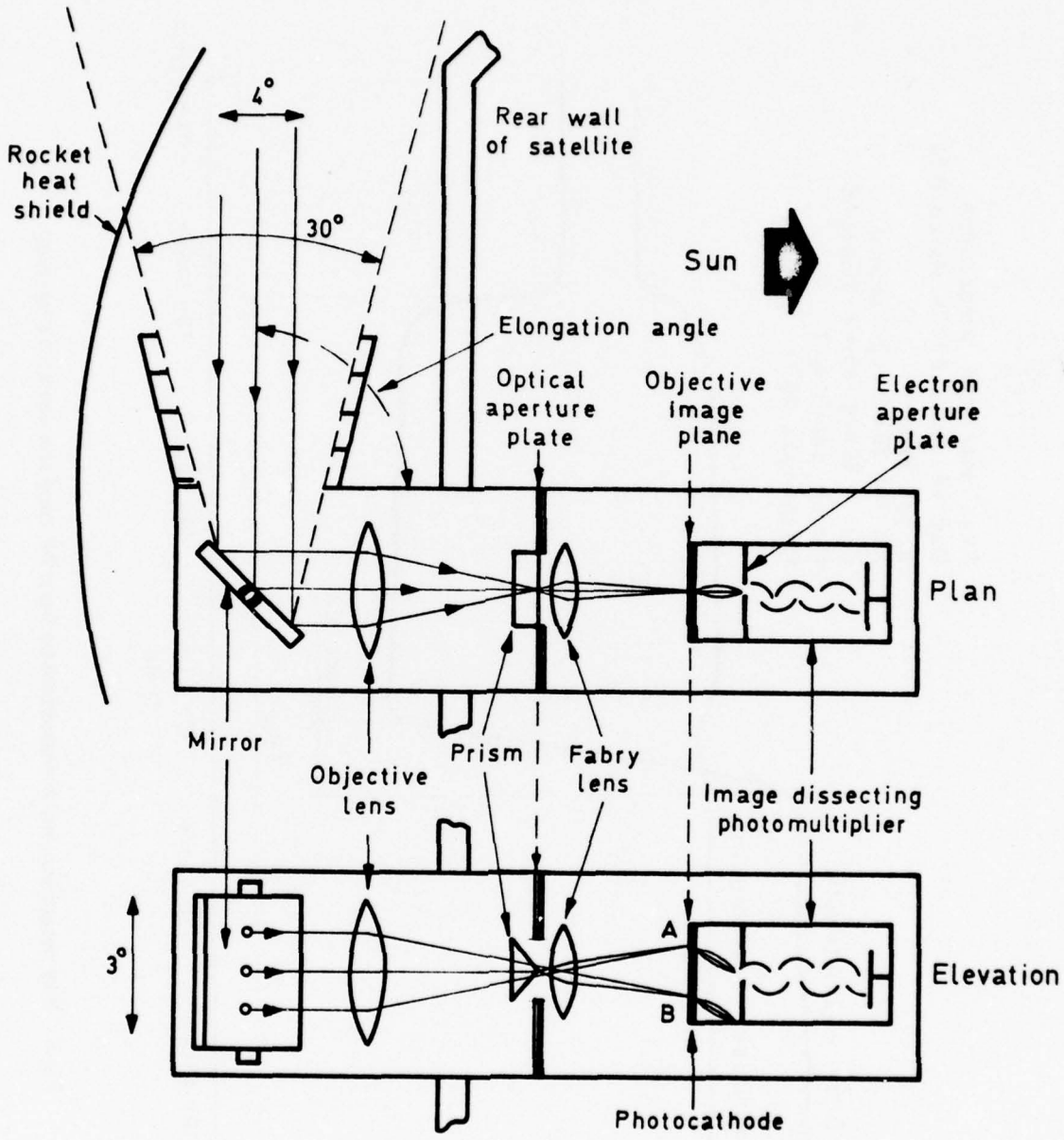

Fig 3 Star sensor schematic

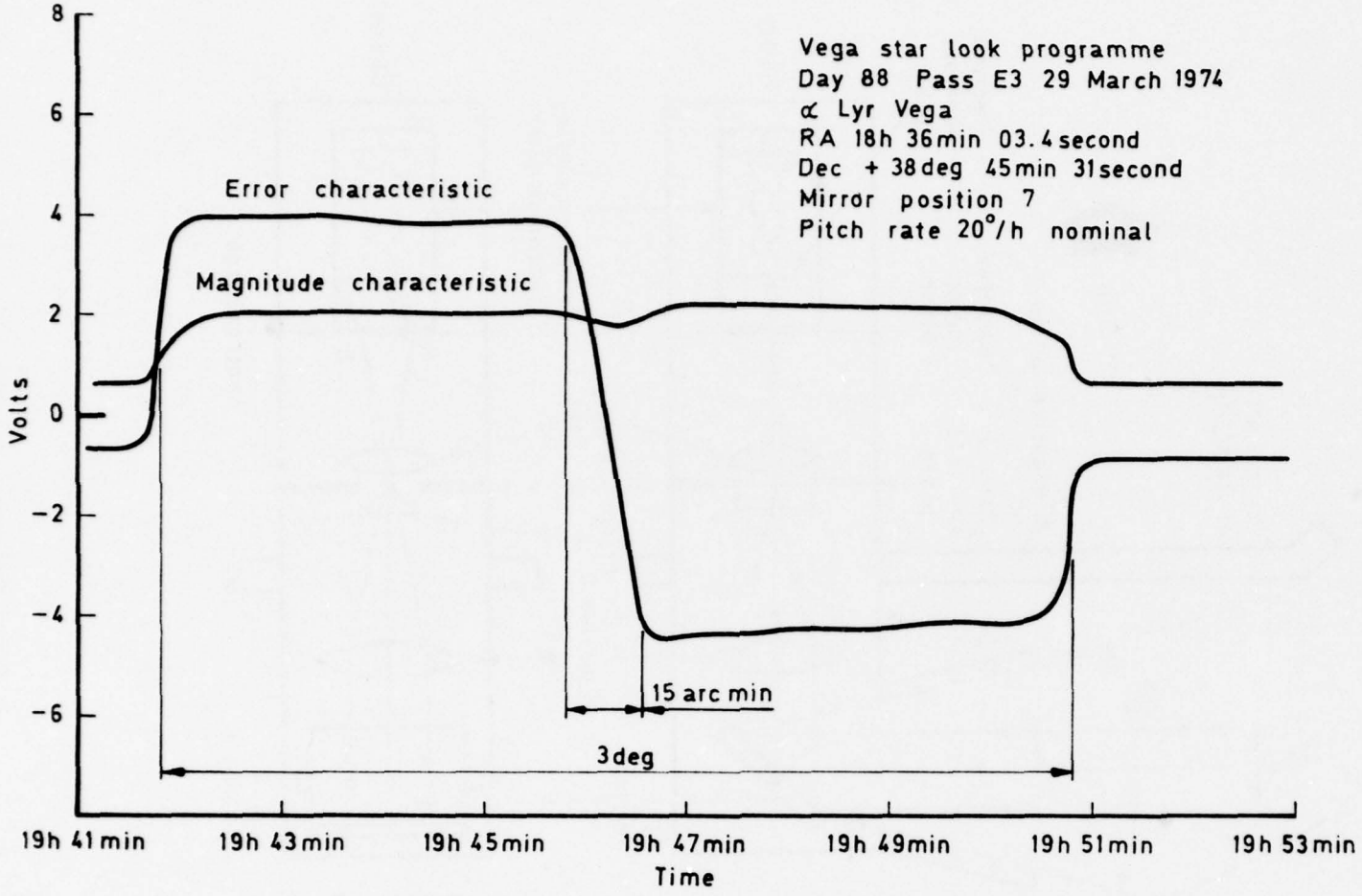

Fig 4 Star magnitude/error characteristic from Miranda star sensor experiment

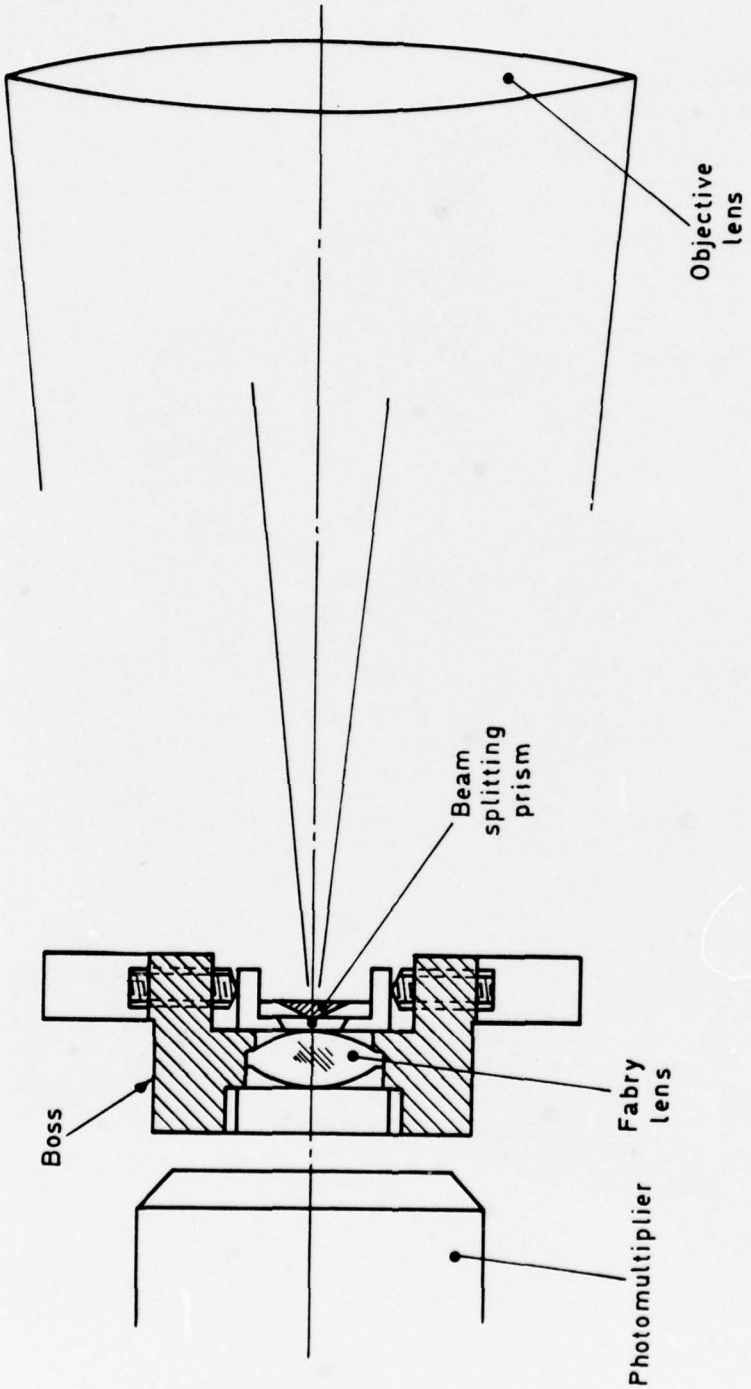

Fig 5 Star sensor optical system

Fig 6

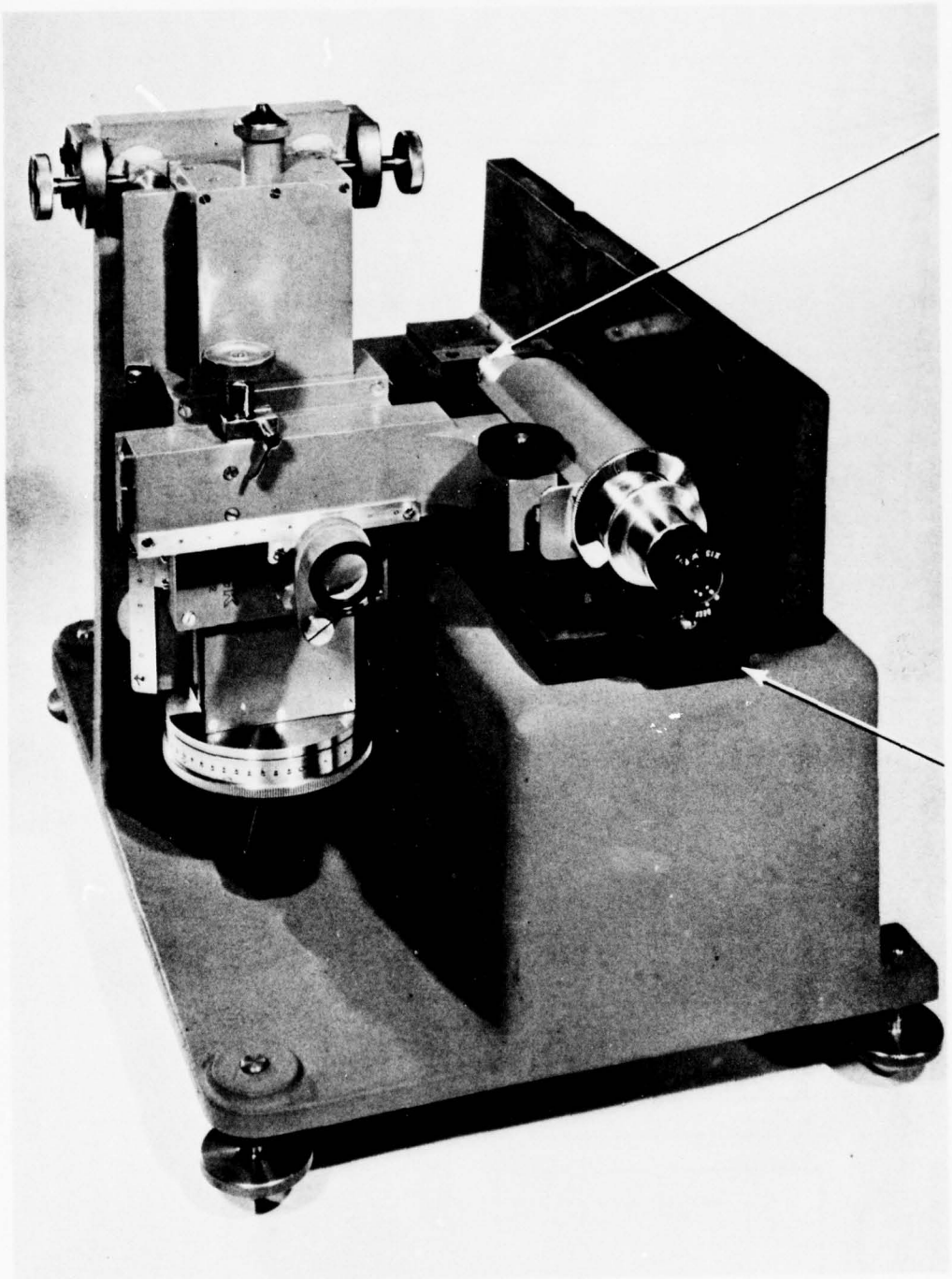

Fig 6 Optical alignment jig

TR 78112 C15055

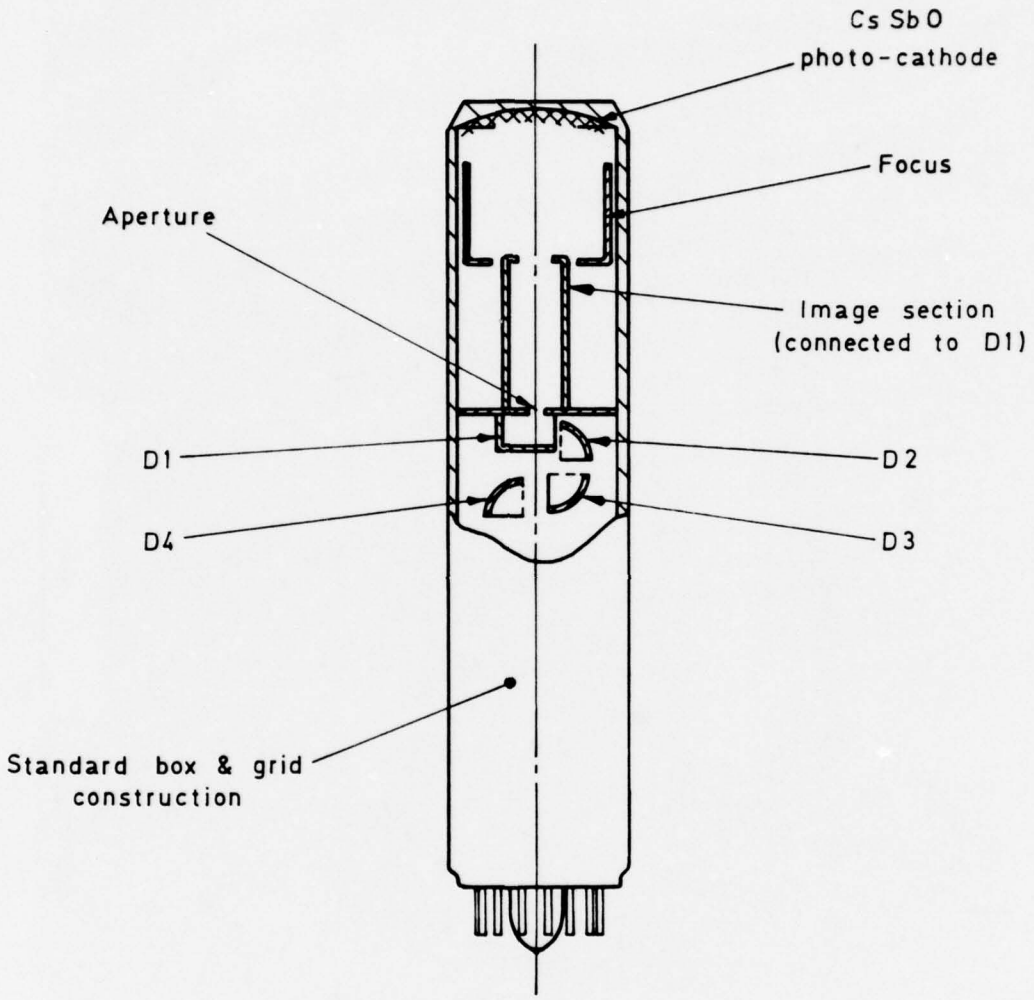

Fig 7 Photomultiplier tube EMI Type D119

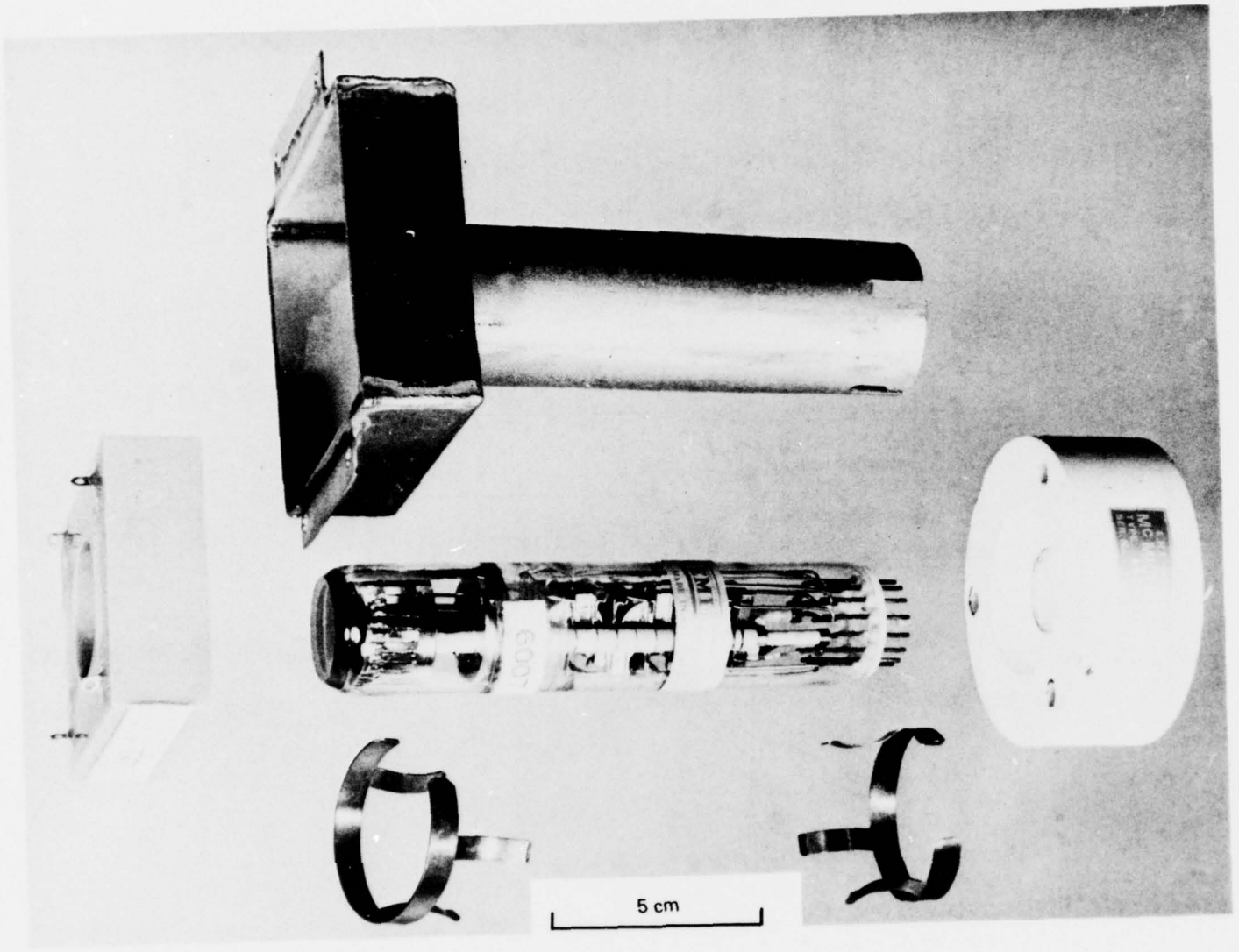

Fig 8 Photomultiplier assembly components

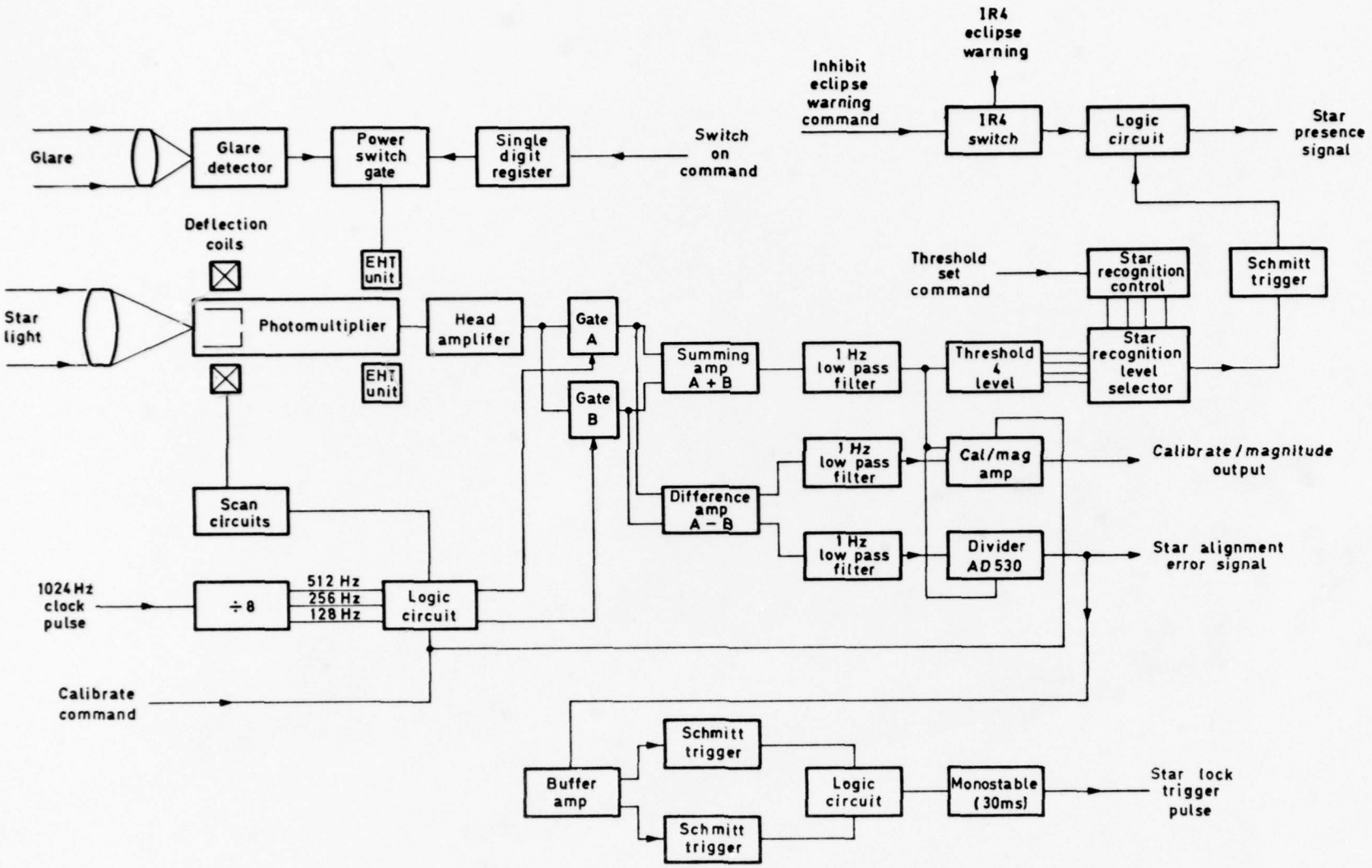

Fig 9 Block diagram of experimental star sensor

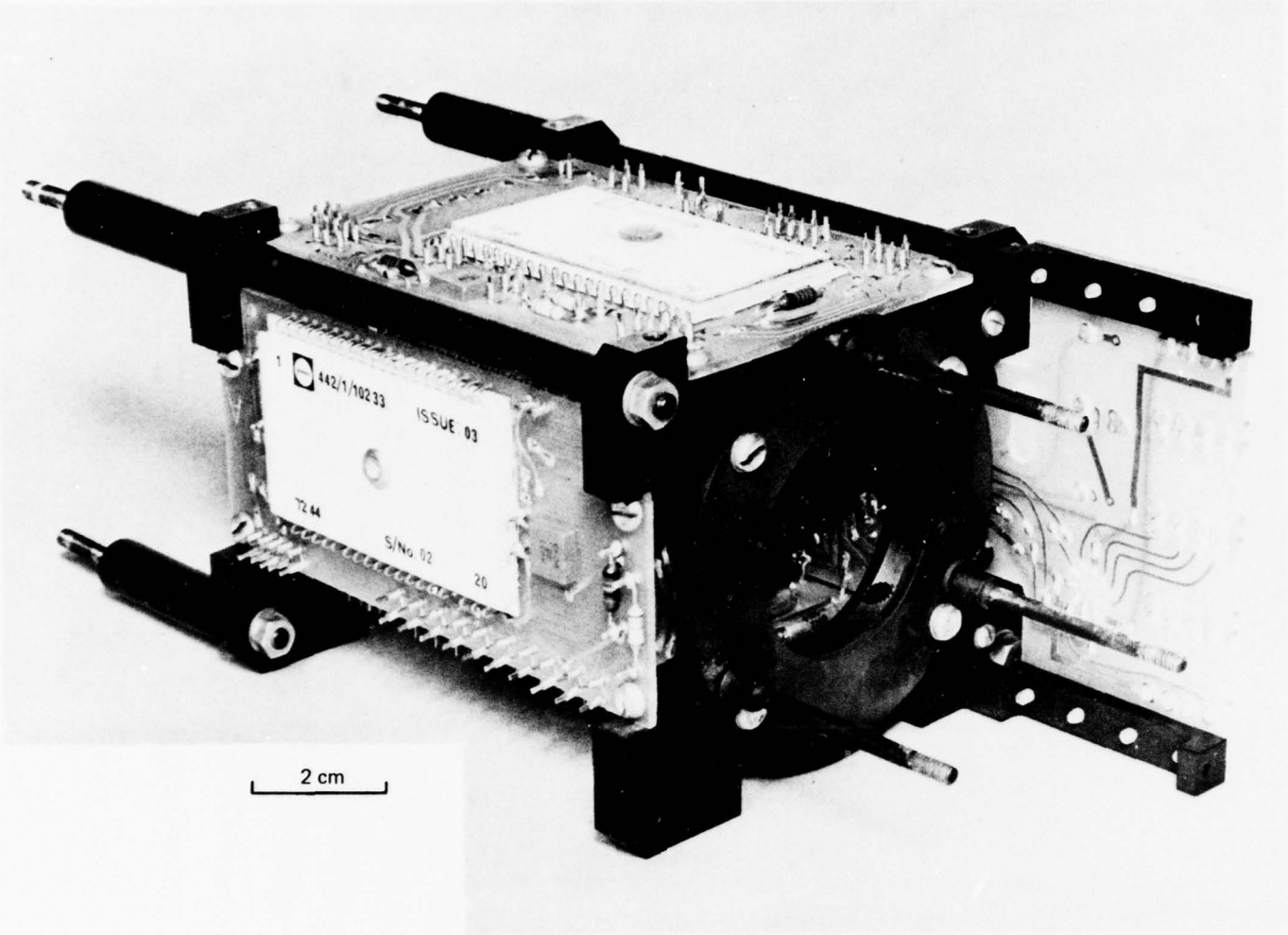

Fig 10 Electronic assembly

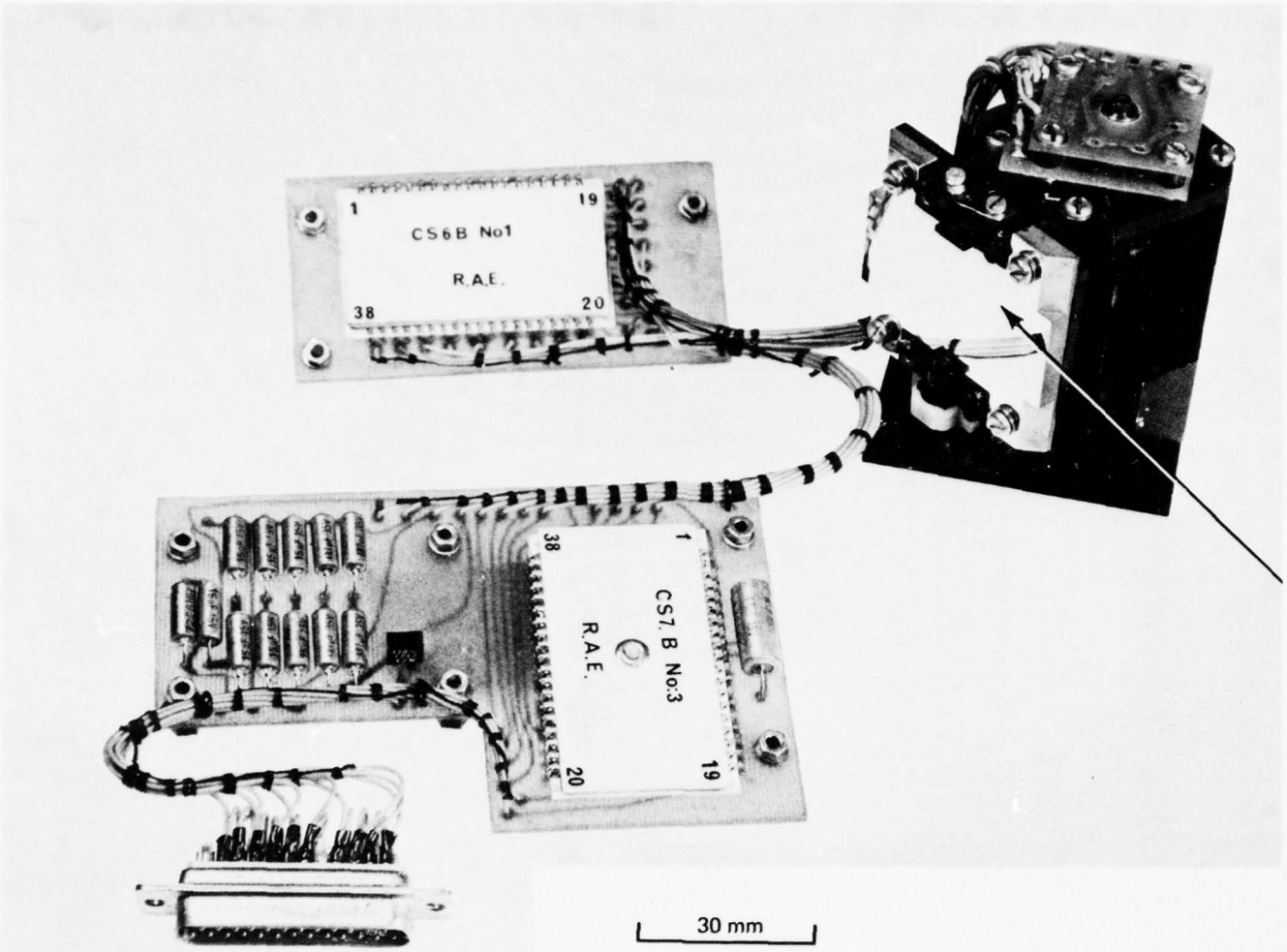

Fig 11 Stepping mirror assembly

Fig 11

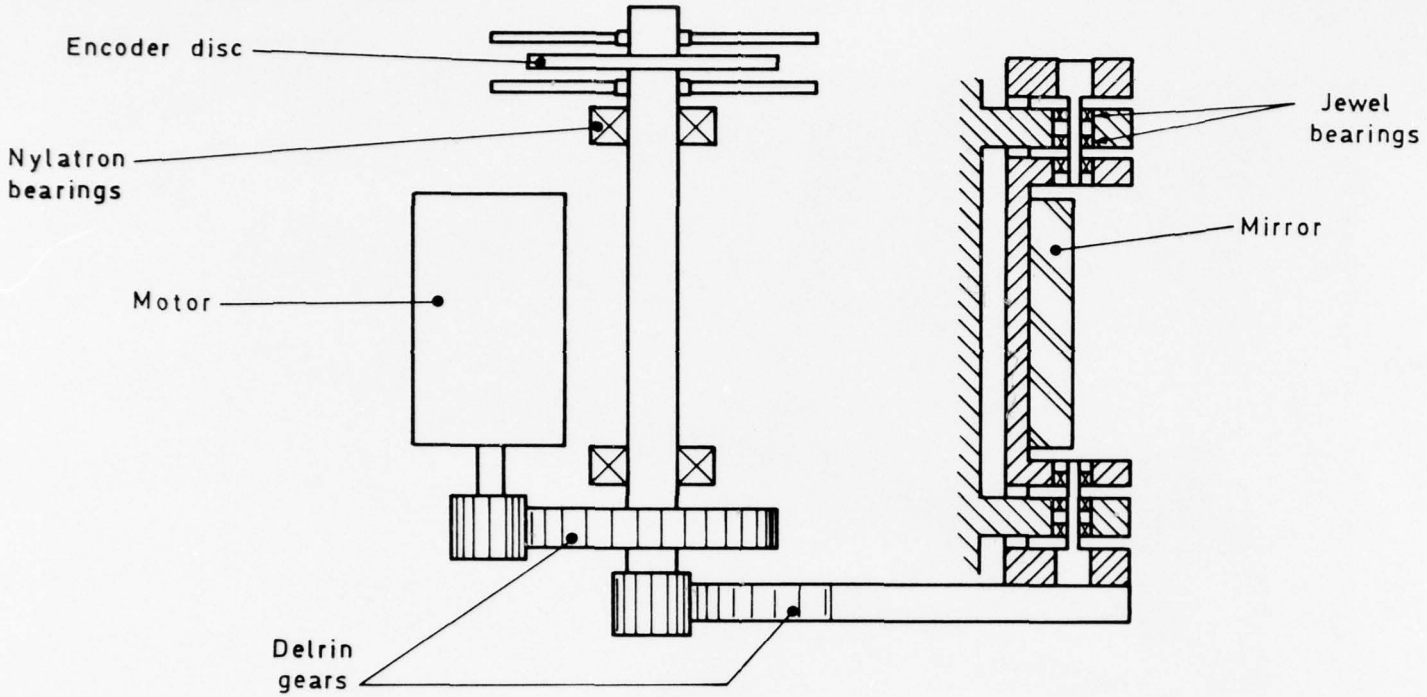

Fig 12 Schematic diagram of stepping mirror mechanism

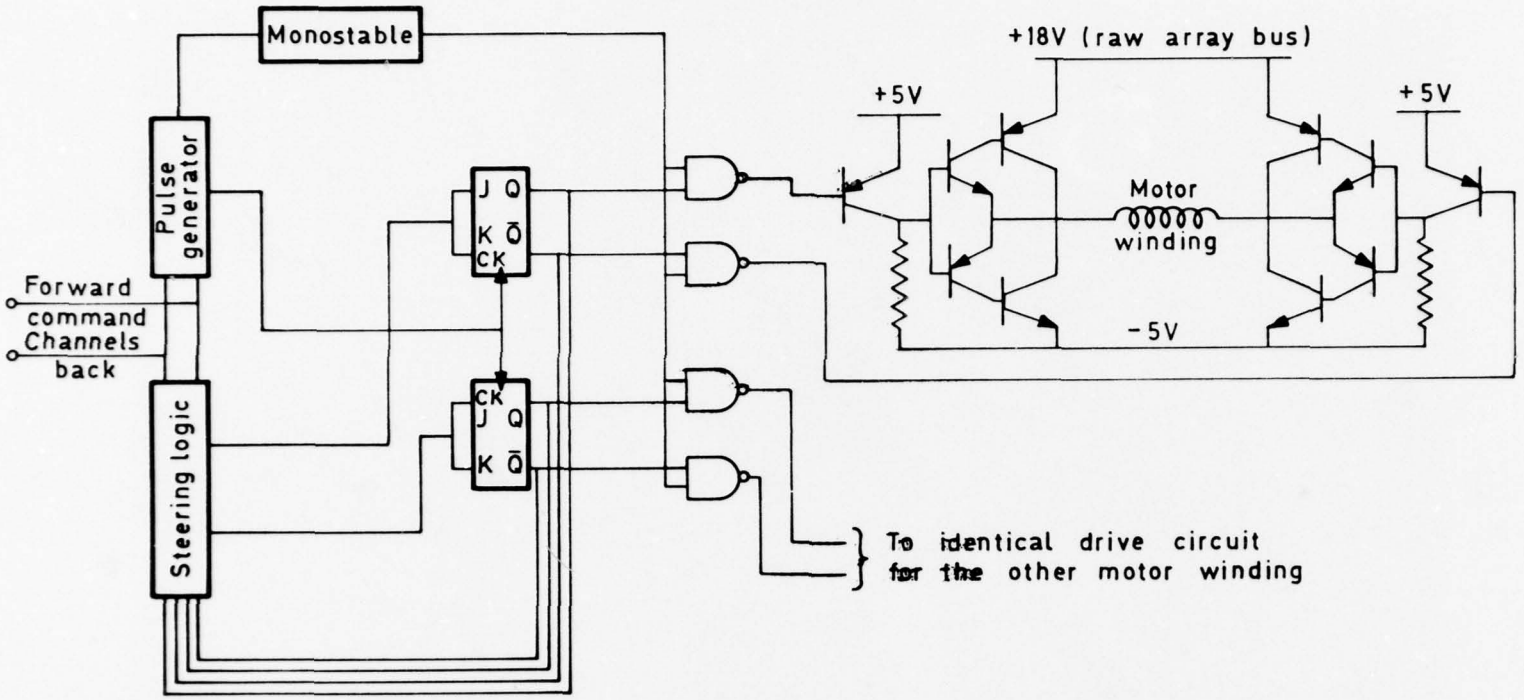

Fig 13 Schematic diagram of mirror drive circuit

Fig 13

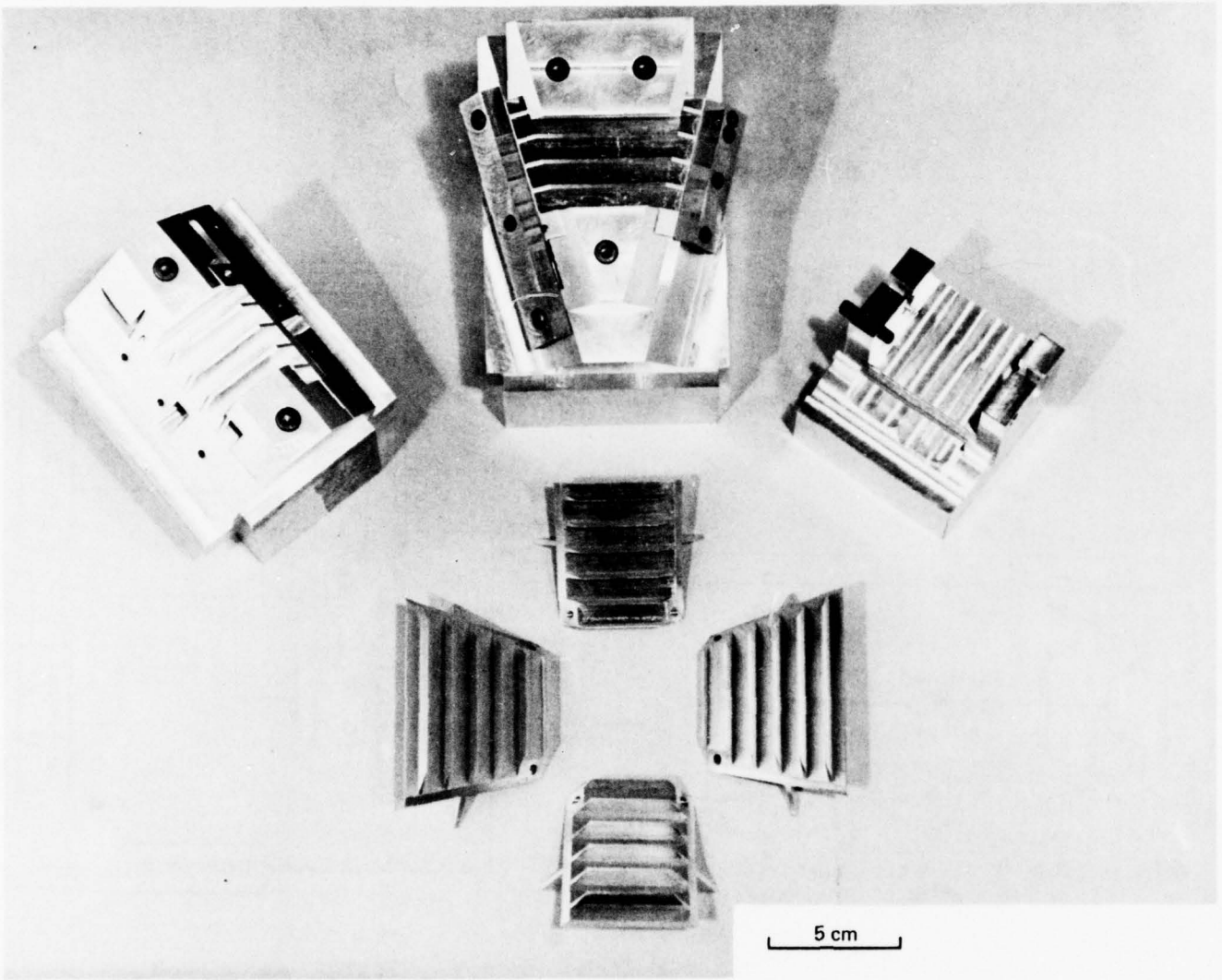

Fig 14 Baffle plates and machining jigs

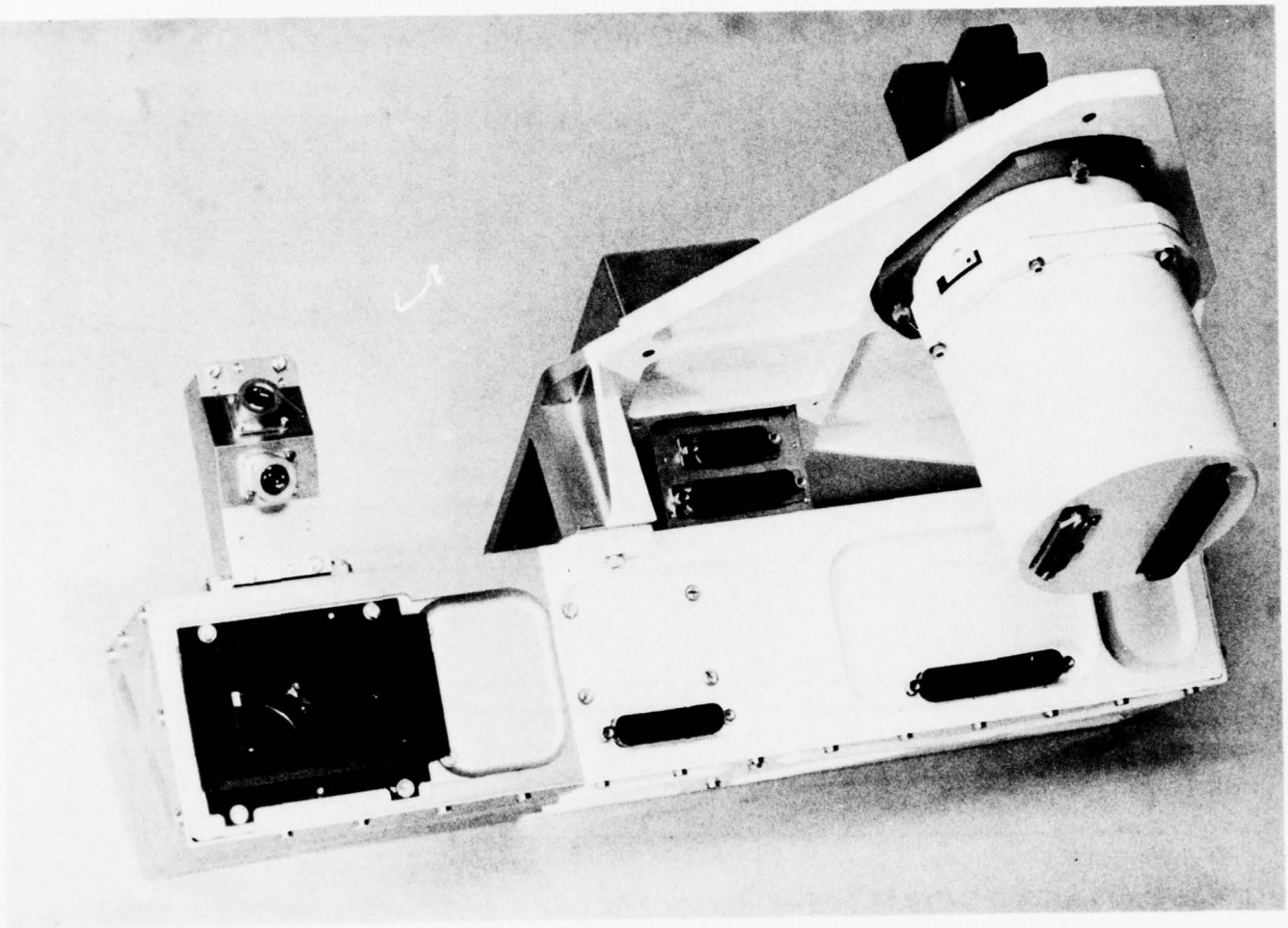

5 cm

Fig 15 Experiment package

Fig 15

Fig 16

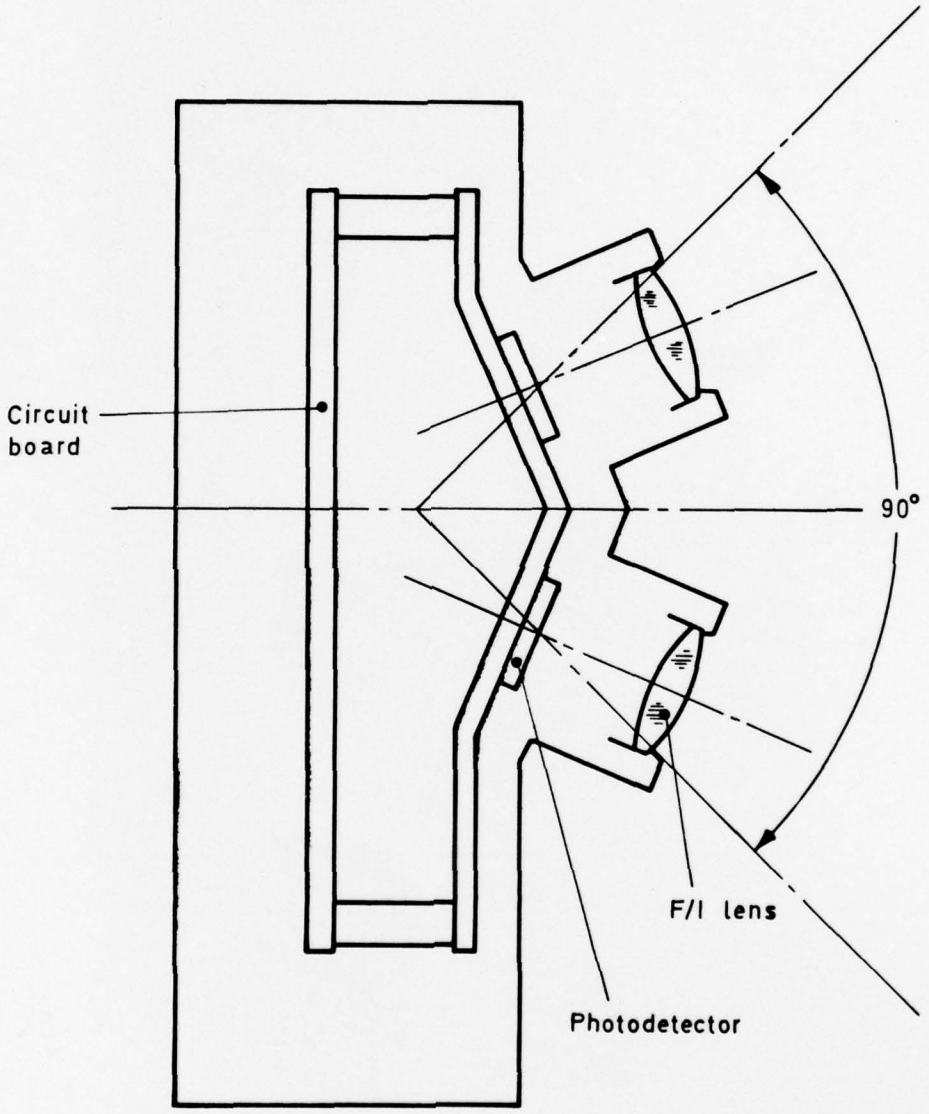

Fig 16 Glare detector optical system

TR 78112

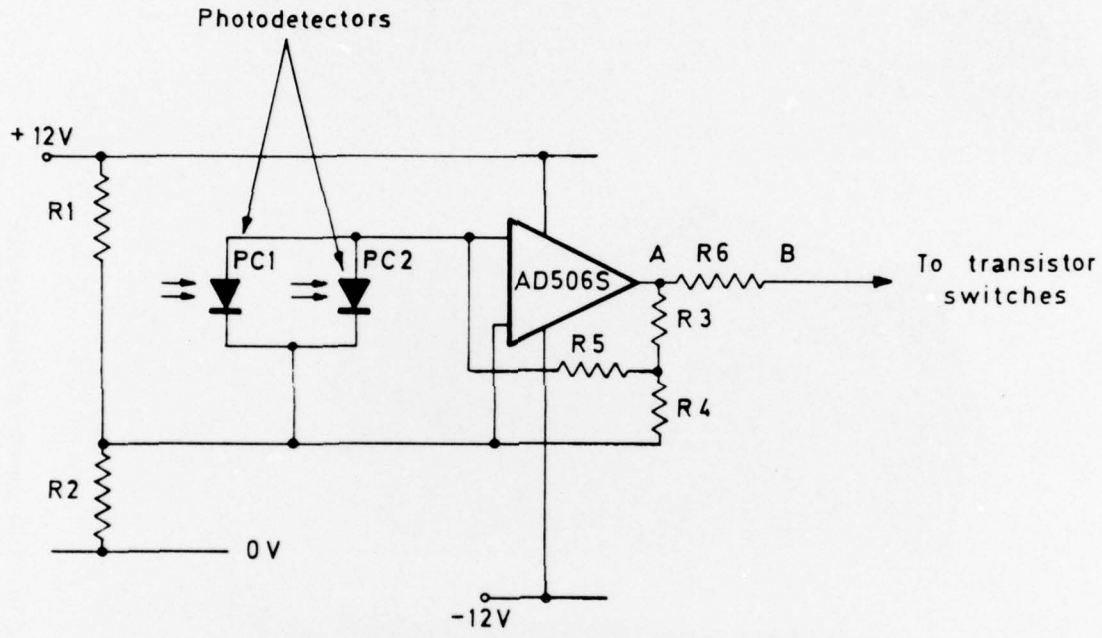

Fig 17 Glare detector circuit

TR 78112

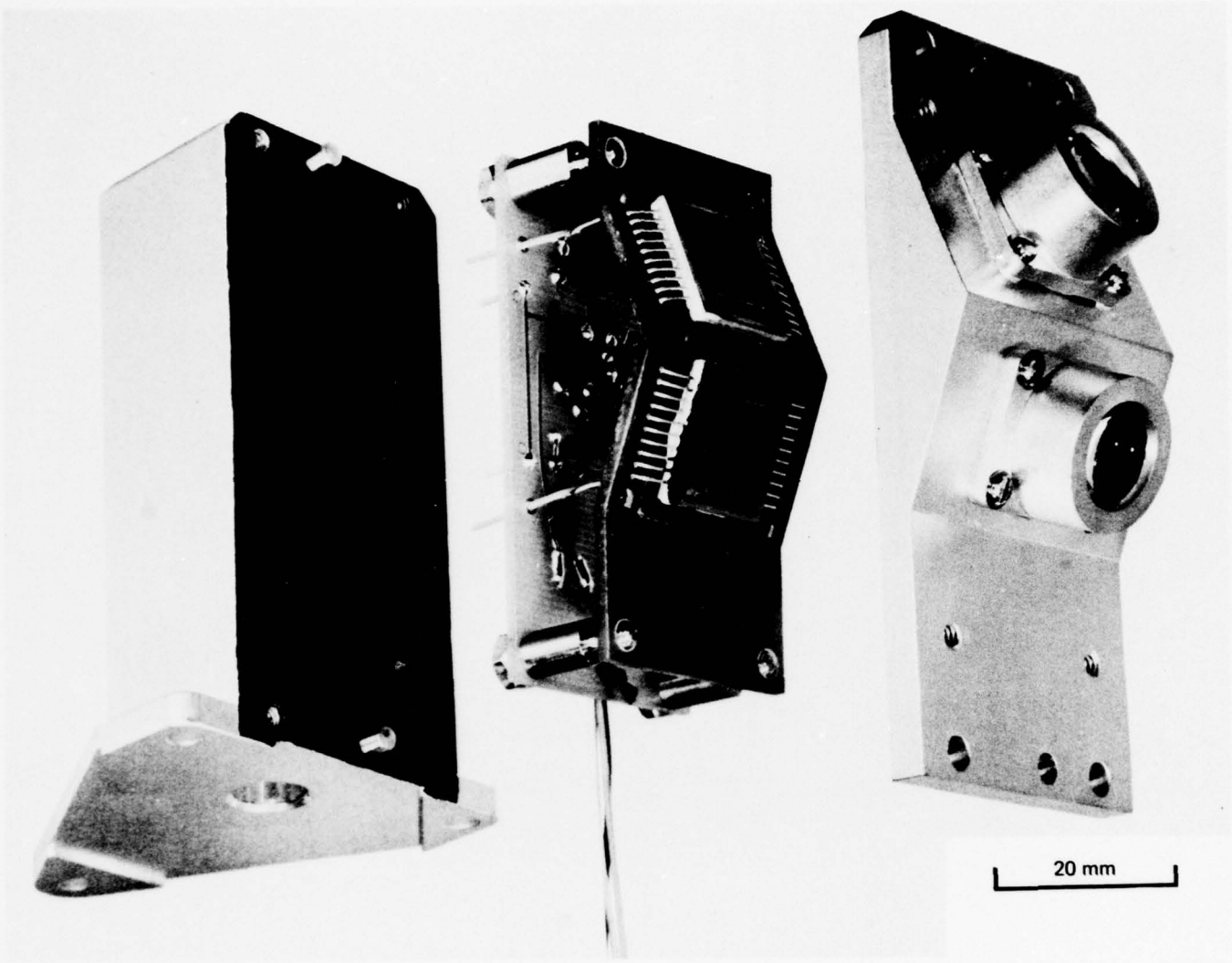

Fig 18 Components of glare detector

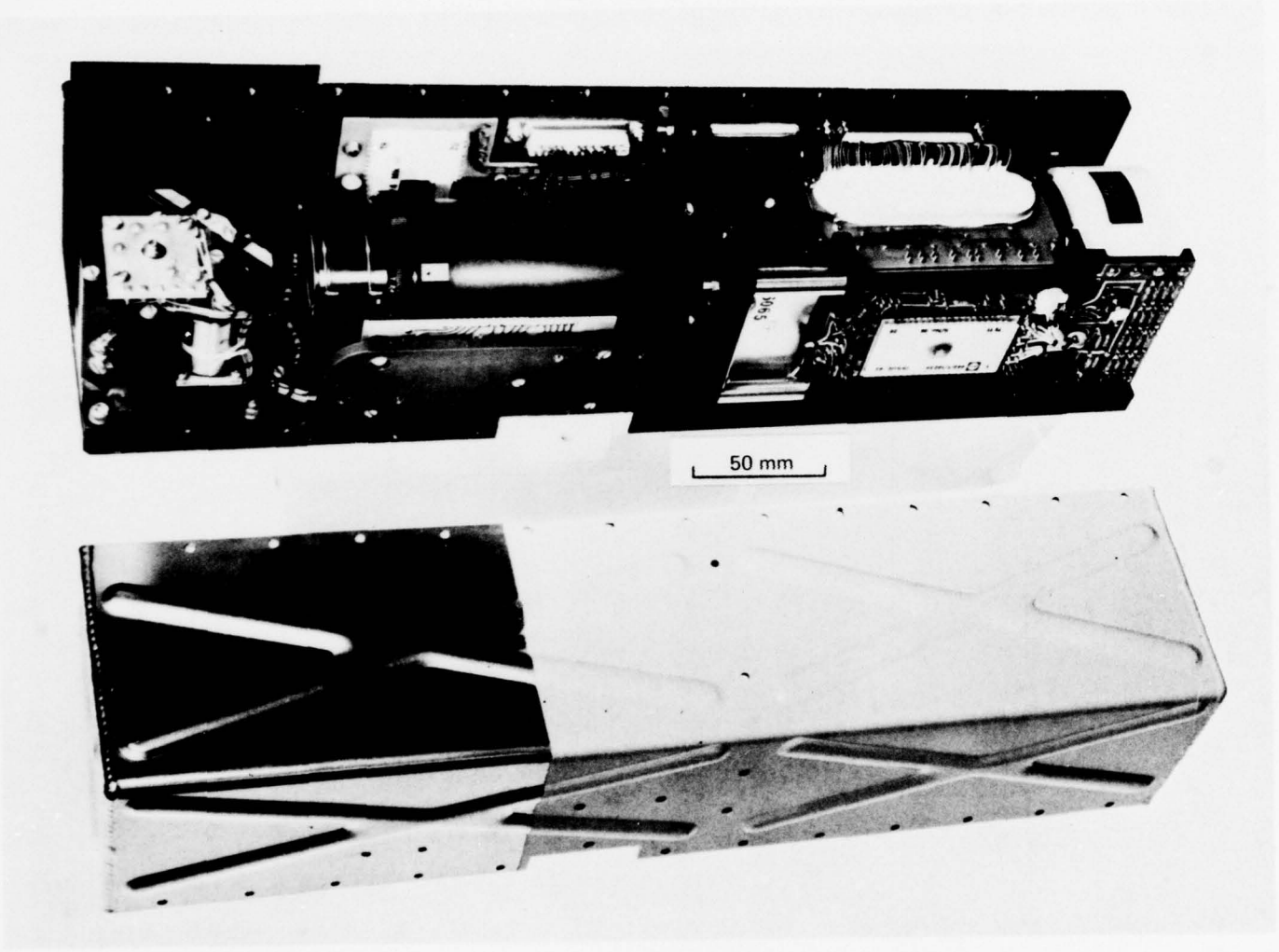

Fig 19 Star sensor assembly

Fig 19

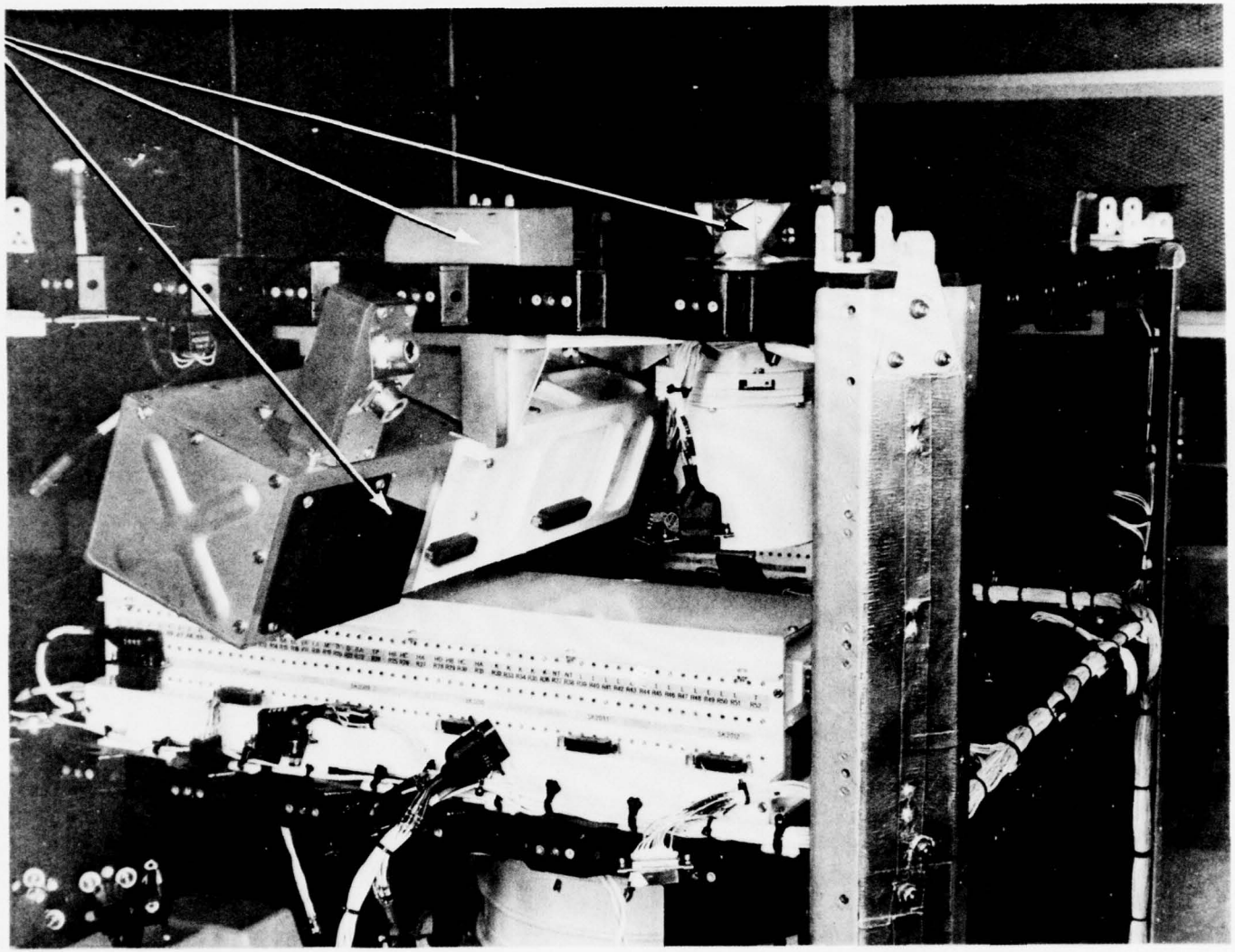

Fig 20 Star sensor mounted in the spacecraft

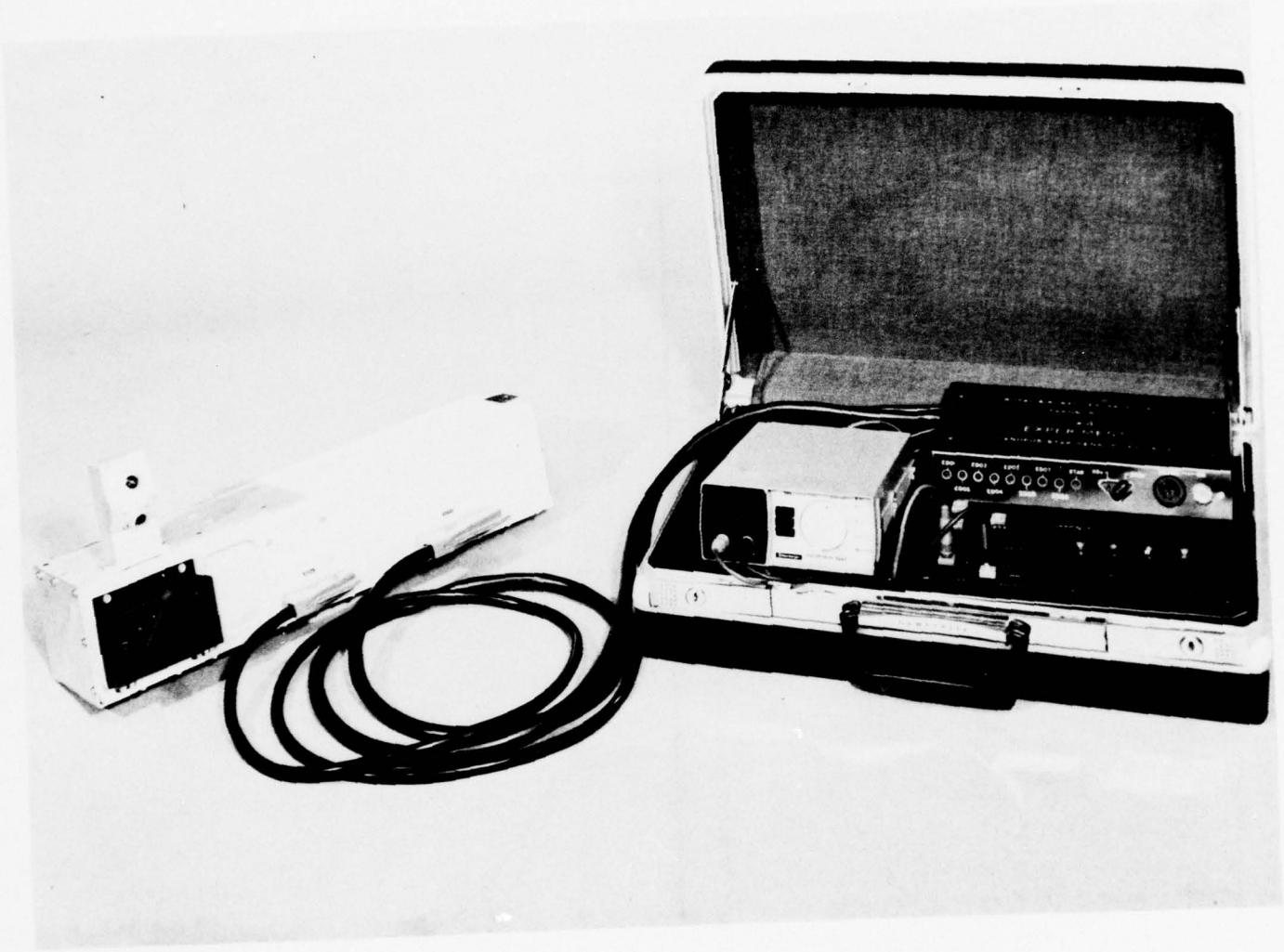

Fig 21 Star sensor with portable test box

Fig 21

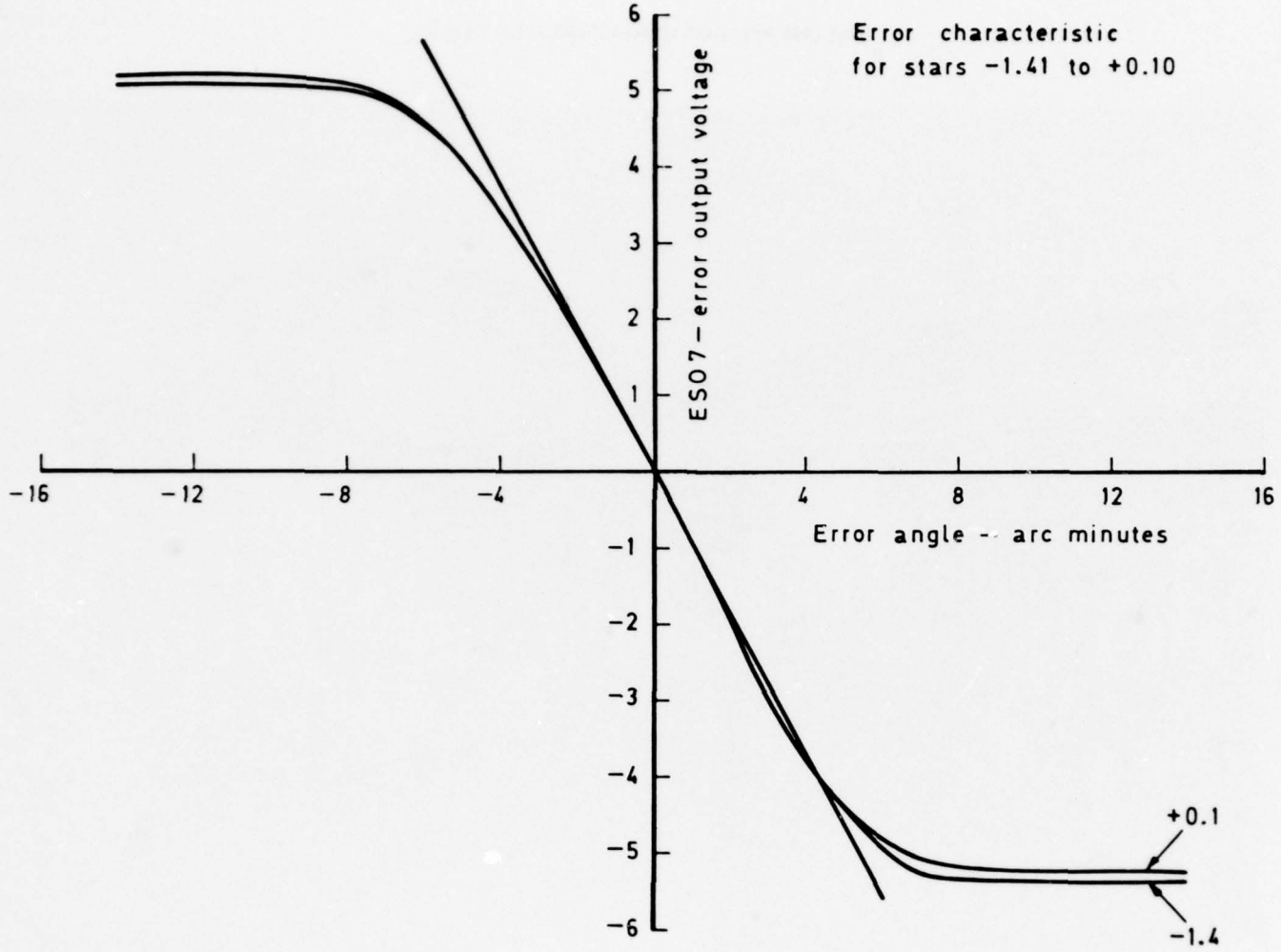

Fig 22 Star sensor error characteristics

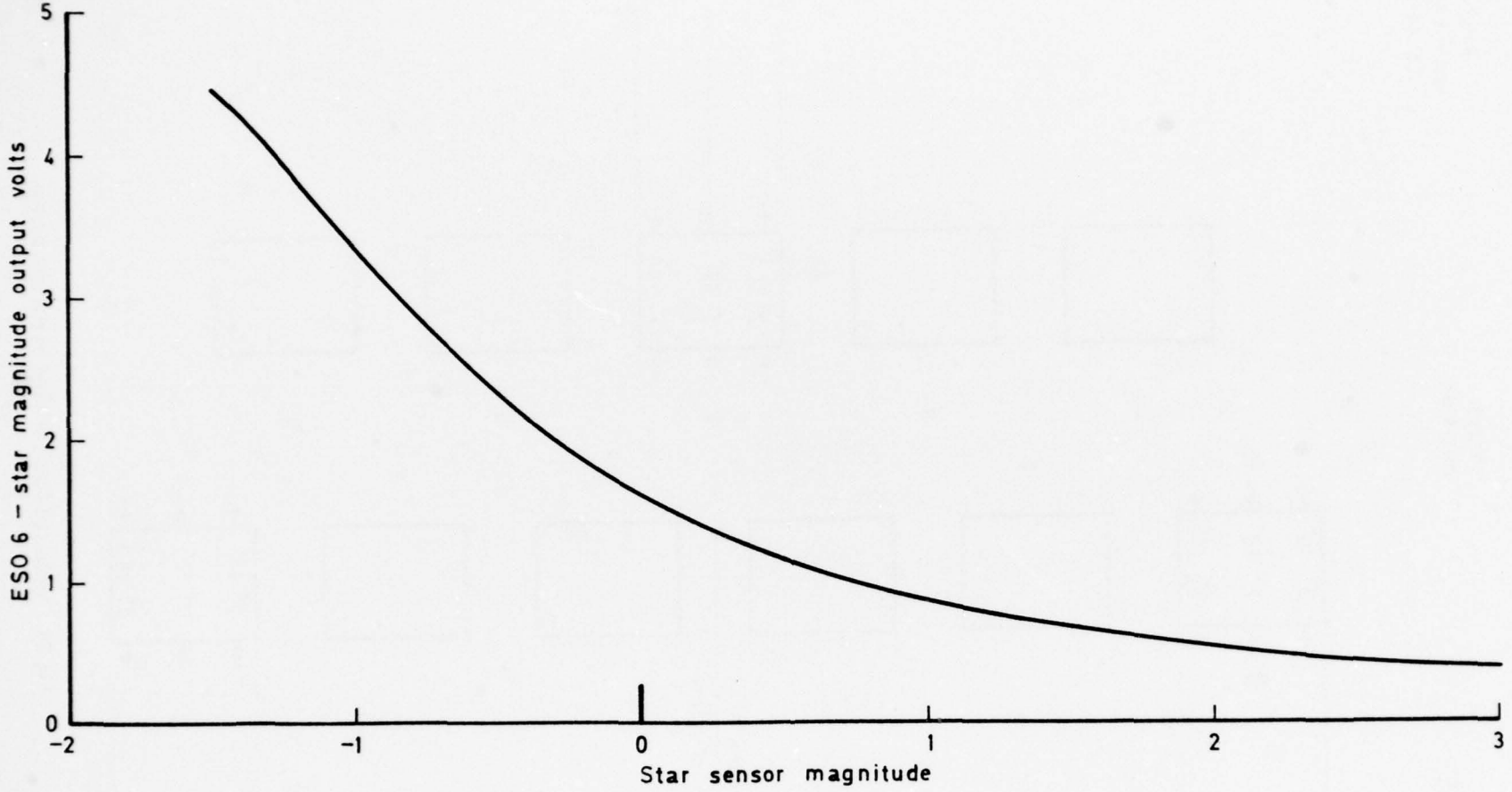

Fig 23 Star magnitude calibration

Fig 23

Fig 24

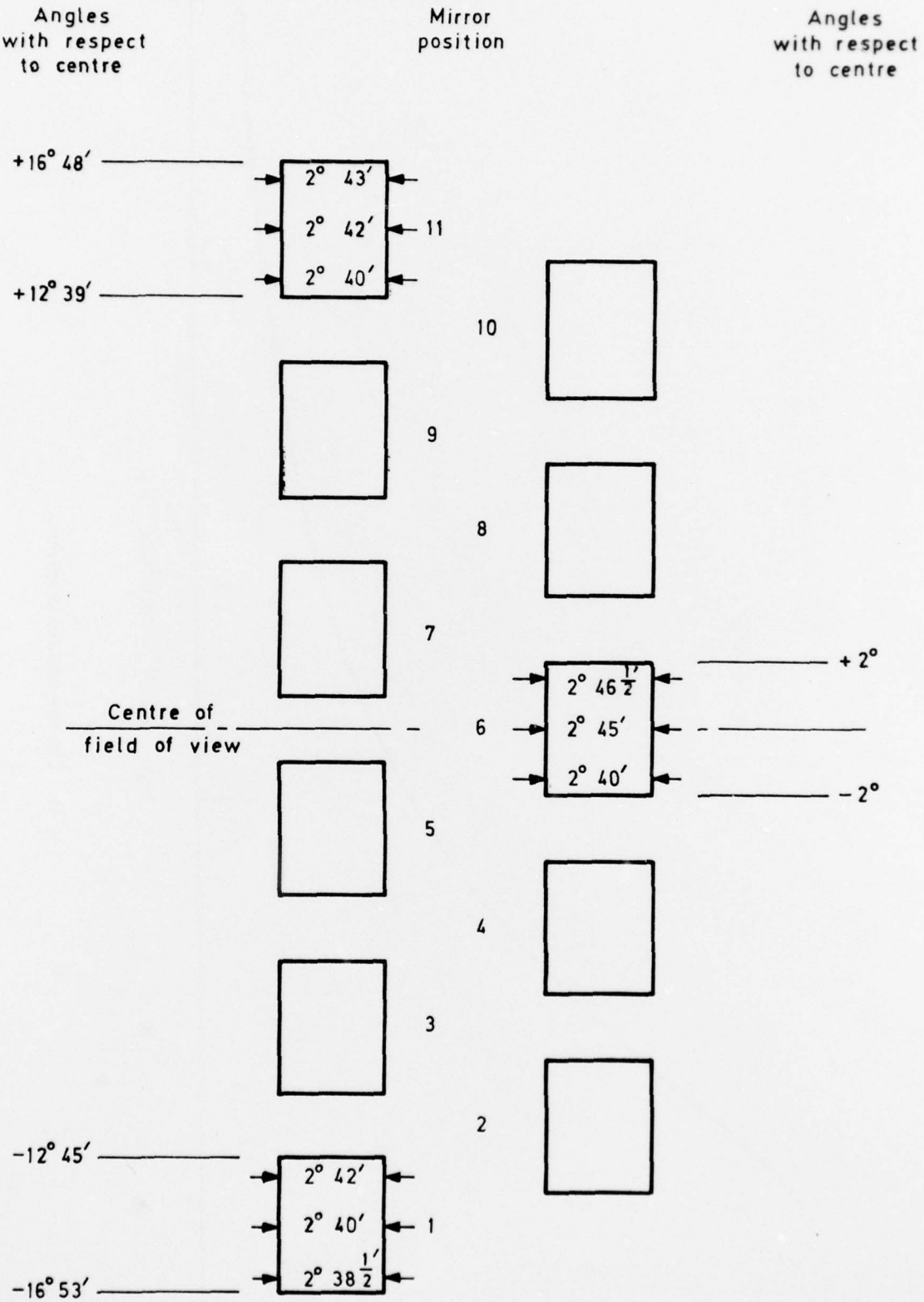

Fig 24 Measured fields of view of the star sensor

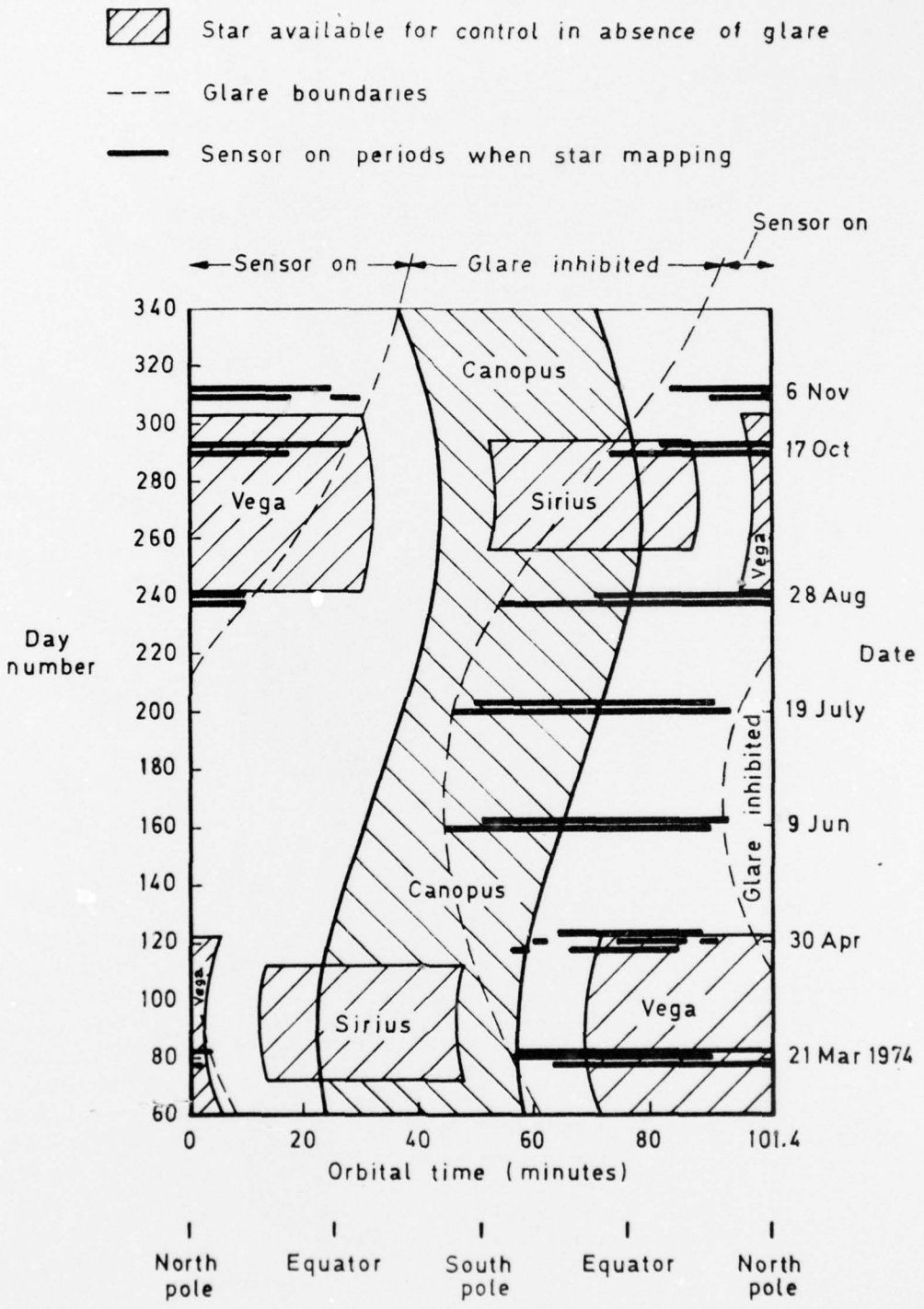

Fig 25 Effect of glare on star availability for attitude control

Fig 26

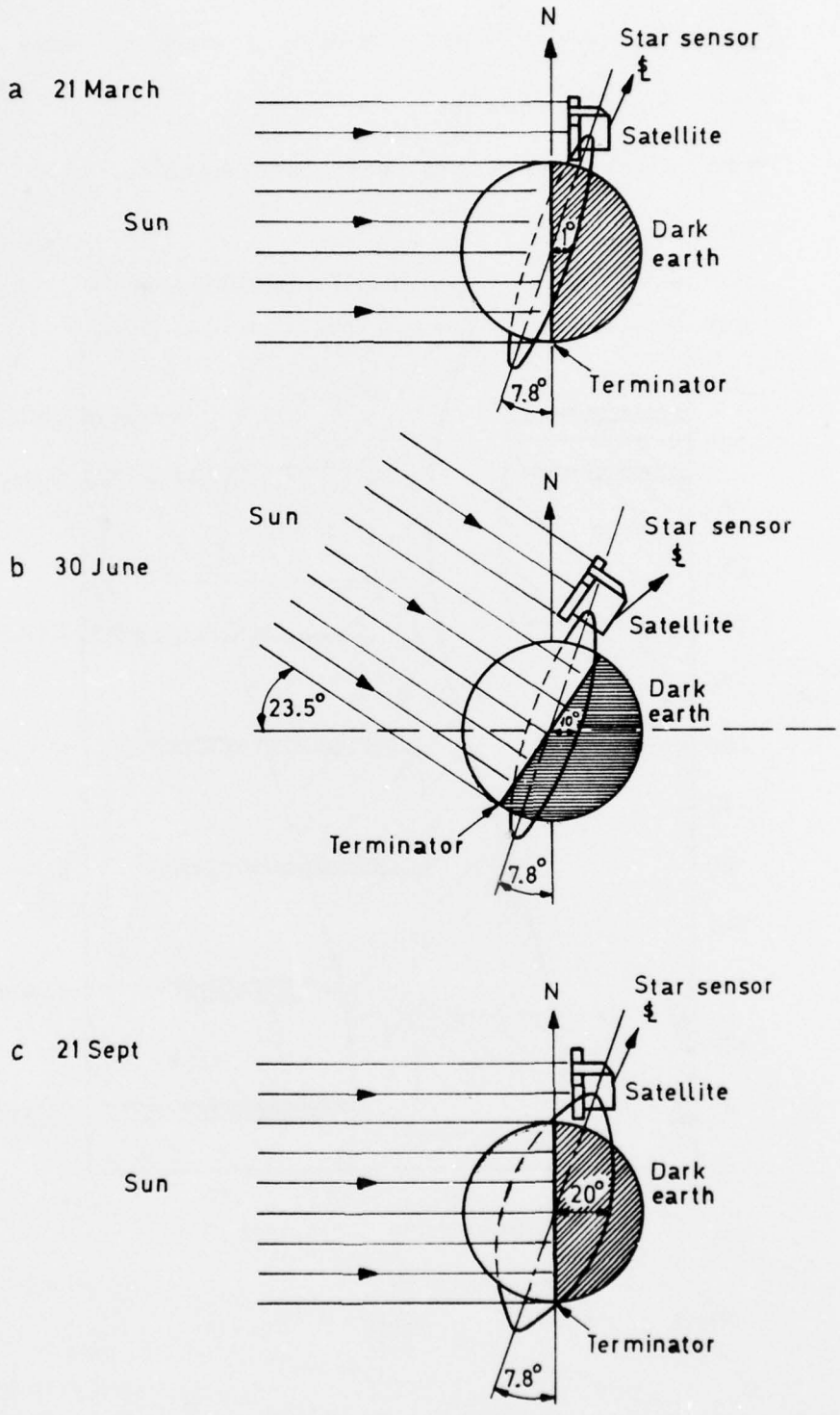

Fig 26 Terminator, orbital plane and satellite attitude relationship during operational life of satellite

TR 78112

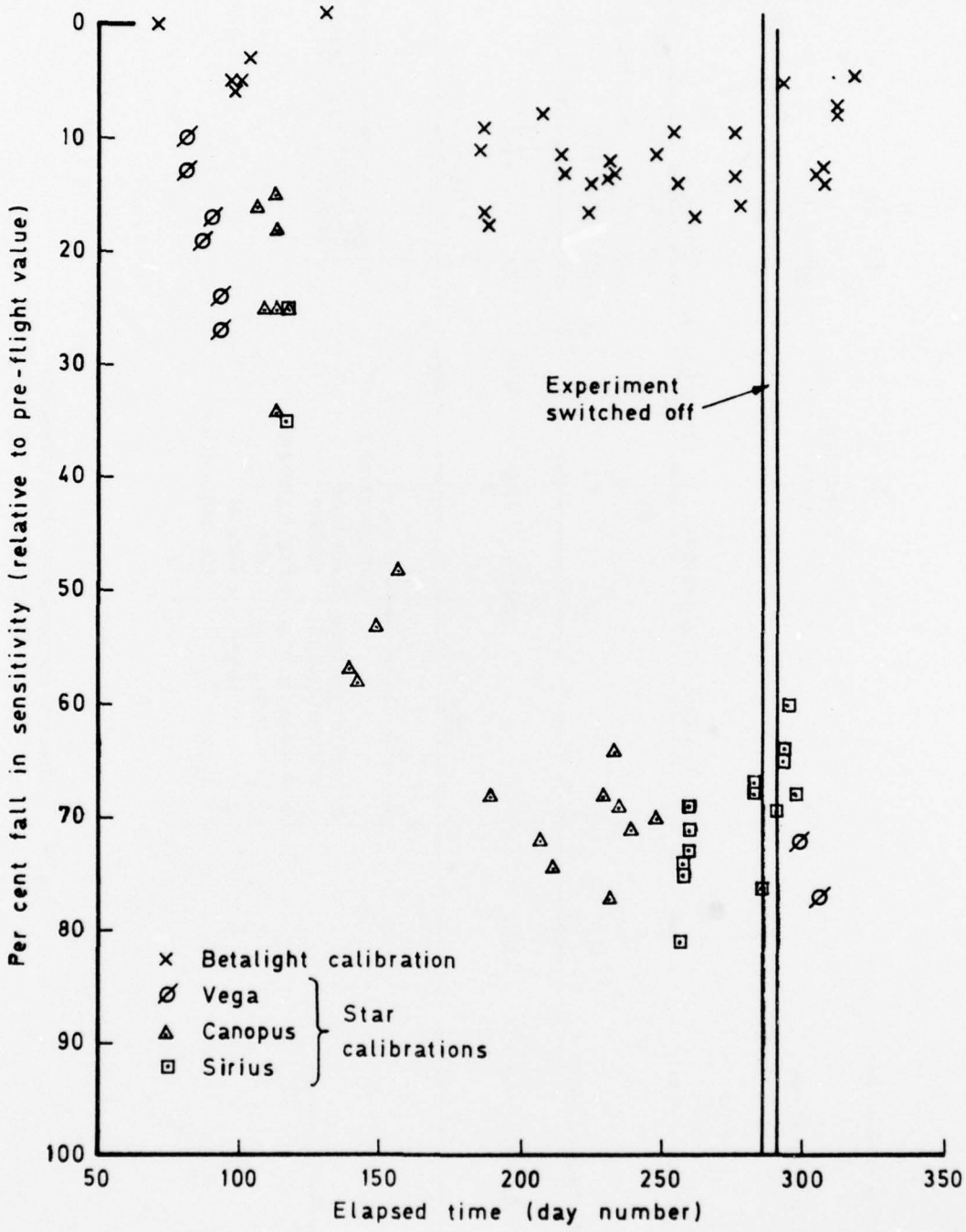

Fig 27 In-flight photometric calibration

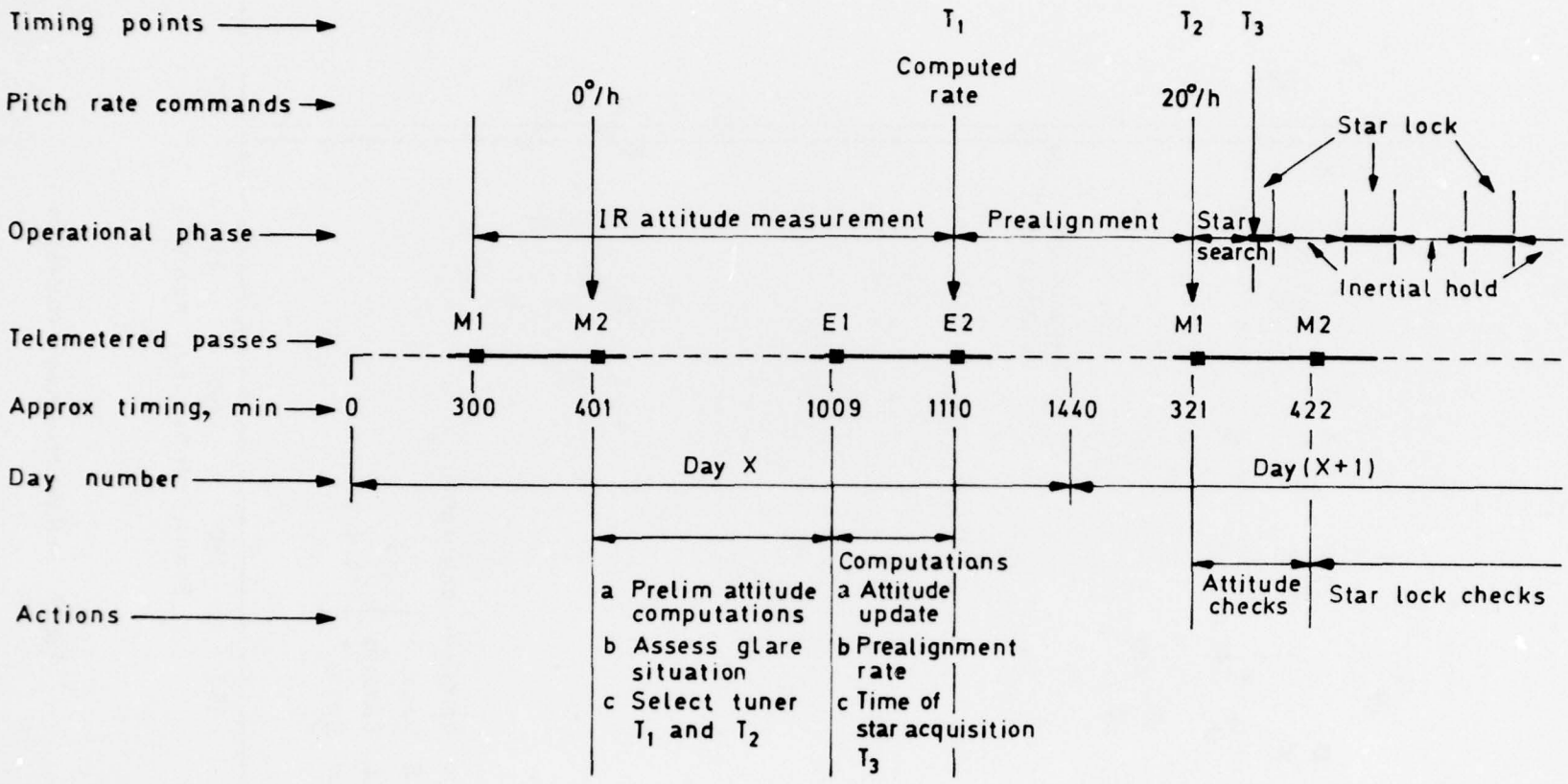

Fig 28 Typical star acquisition and lock procedure

REPORT DOCUMENTATION PAGE

Overall security classification of this page

UNCLASSIFIED

As far as possible this page should contain only unclassified information. If it is necessary to enter classified information, the box above must be marked to indicate the classification, e.g. Restricted, Confidential or Secret.

1. DRIC Reference (to be added by DRIC)	2. Originator's Reference	3. Agency Reference	4. Report Security Classification/Marking
	RAE TR 78112	N/A	UNCLASSIFIED

5. DRIC Code for Originator	6. Originator (Corporate Author) Name and Location
850100	Royal Aircraft Establishment, Farnborough, Hants, UK
5a. Sponsoring Agency's Code	6a. Sponsoring Agency (Contract Authority) Name and Location
N/A	N/A

7. Title The Miranda star sensor experiment

7a. (For Translations) Title in Foreign Language

7b. (For Conference Papers) Title, Place and Date of Conference

8. Author 1. Surname, Initials	9a. Author 2	9b. Authors 3, 4	10. Date	Pages	Refs.
Brown, G.W.	Haskell, P.	Hollaway, B	September 1978	70	18

11. Contract Number	12. Period	13. Project	14. Other Reference Nos.
N/A	N/A	X4.	Space 558

15. Distribution statement

(a) Controlled by – [redacted]

(b) Special limitations (if any) –

16. Descriptors (Keywords) (Descriptors marked * are selected from TEST)

Miranda. X4. Star sensors. Photomultiplier. Attitude control.

17. Abstract

This is an account of the star sensor experiment in Miranda, the British technology satellite launched by an American Scout rocket from Vandenberg AFB, California in March 1974. The star sensor used in this experiment is a single axis sensor and was designed and built at the RAE. The main aims of the experiment were to investigate the performance of the sensor in orbit and to demonstrate its compatibility with the spacecraft attitude control system when used to track a star.

The authors describe the basic design features of the sensor and the methods used to test and integrate it with the satellite. They outline the various attitude control modes that were available in orbit and describe the way these were used to acquire and lock the control system onto the selected star. The aperture of the sensor's objective lens was only 2.5 cm in diameter and although some scattered earth albedo interference occurred, many crossings of stars down to +4.5 detector magnitude were recorded during the star mapping exercises and six successful star locks were achieved on either Canopus or Sirius at roughly one month intervals, during the 8 month operational lifetime of the satellite. On each of these occasions the control system remained in lock for its full scheduled period of about 2 days and only unlocked when commanded to do so.

F5910/1

RAE Form A143